Particle Accelerators, 1970, Vol. 1, pp. 285–310

NEW USES FOR LOW-ENERGY ACCELERATORS†

P. D. PARKER‡

Wright Nuclear Structure Laboratory, Yale University, New Haven, Connecticut, U.S.A.

The areas of Nuclear Astrophysics, Beam-Foil Spectroscopy, and Solid-State Physics are discussed as examples of interdisciplinary fields where there is exciting and important research which is accessible to low-energy accelerators and which is ripe for harvest by workers with training in nuclear physics techniques and with interest in these areas of the scientific frontier. Along with a presentation of the concepts and the important problems in these areas, the techniques and hardware necessary for research in these areas are also described and discussed.

1. INTRODUCTION

While there is still a clear need for larger and more powerful accelerators to extend our knowledge of subatomic physics, it is now becoming apparent that it is also important to find efficient ways for utilizing many of the smaller, low-energy accelerators that are seemingly left behind in the mad rush toward the newer and more glamorous facilities. It we arbitrarily define low-energy accelerators as those producing beams with maximum singly-charged particle energies of $\leqslant$6 MeV, we include in this 'left behind' classification 229 accelerators in the United States of which 112 are located at universities and colleges, 64 at industrial laboratories, and 53 at government laboratories. These facilities involve roughly 250 graduate students and 320 faculty members at the academic locations and comparable research staffs at the industrial and governmental laboratories.

With this in mind, an ad hoc panel was established in 1968 by the Committee on Nuclear Science of the NRC-NAS to examine new uses for these low-energy accelerators. This panel included in its membership W. A. Fowler (chairman), S. Bashkin, D. Bodansky, W. L. Brown, D. D. Clayton, J. A. Davies, D. B. Fossan, J. W. Mayer, P. D. Parker, W. E. Stephens, W. Whaling, and E. A. Wolicki. In their report this panel emphasized the belief that great discoveries in science can still be made with modest means, pointing out that there is still important nuclear structure work to be done with these machines and examining in detail the important interdisciplinary research which can be done by applying these facilities to the areas of nuclear astrophysics, atomic physics, and solid-state physics. The following text has been prepared as a summary of the panel's report[1] which was originally published in December, 1968. References have been given to specific manufacturers or to specific publications that exemplify particular instruments or techniques. These references are *not* intended to be complete, and the choice of referenced manufacturers and publications does *not* represent the result of a careful, comparative evaluation; in most cases these are simply examples which happen to be conveniently accessible or familiar to the authors of this report. The references to industrial organizations are included, because these organizations undoubtedly constitute a primary resource of knowledge and sophistication concerning the instruments under discussion and their uses, existing and potential. The specific organizations referenced are not always necessarily the single best, or even the only, sources of sound experience and information. Undoubtedly, there are many of equal competence not named simply because of the constitution of the panel and its experience. In its report the panel has attempted to be understood by all prospective readers, and thus we make no apologies to the experienced researcher for describing subjects already familiar to him.

Before plunging into the reorientation of an accelerator facility along the lines suggested by the panel, it must be cautioned that special devotion and dedication are required . . . new fields and concepts must be explored and new techniques must be learned. Recognizing these challenges, however, the panel feels that real and significant contribu-

† Summary of the report by the NRC-NAS ad hoc Panel on New Uses for Low-Energy Accelerators which was supported jointly by the National Academy of Science, the National Science Foundation, the Office of Naval Research and the U.S. Atomic Energy Commission.

‡ This summary was prepared at the request of the Editor of *Particle Accelerators*. The members of the original panel included W. A. Fowler (Chairman), S. Bashkin, D. Bodansky, W. L. Brown, D. D. Clayton, J. A. Davies, D. B. Fossan, J. W. Mayer, P. D. Parker, W. E. Stephens, W. Whaling and E. A. Wolicki.

tions to these frontier fields of science will amply justify the required effort. Furthermore, at a time of stagnating funding budgets when the prospects for obtaining major new equipment are dim it would not be improper to view these suggestions as appropriate ways for expanding our scientific horizons in spite of budgetary limitations.

2. NUCLEAR ASTROPHYSICS

The application of nuclear physics to problems in astrophysics consists of ascertaining which nuclear reactions are of importance and of measuring the relevant nuclear data—primarily cross sections. General astrophysical theory can delineate the potential importance of specific reactions, but painstaking laboratory experiments are required to establish quantitatively their significance within the astrophysical scheme. The desired cross sections are among the smallest measured in the low-energy nuclear laboratory. Long integration times and careful attention to background counts are common necessities. From a purely nuclear point of view, moreover, the reactions studied are often of comparatively little interest. The intellectual stimulation is more to be found in wresting from nature a hard-won number that she herself has presumably used and in evaluating its astrophysical consequences. An investigator not sharing this interest will be little amused by his task. The nuclear physicist interested in astrophysics, on the other hand, will find many advantages to this type of research: it is an excellent vehicle for entering an exciting field of research on a learn-as-you-go basis; it requires an assimilation of basic laboratory technique with the associated benefit of student training; and it can be relatively inexpensive for those having access to a low-energy accelerator.

In nuclear astrophysics the primary role of low-energy accelerators is the measurement of the nuclear reaction cross sections which are necessary for the evaluation of thermonuclear reaction rates at the various stages of stellar evolution.[2-6] The relevant energy for these measurements should correspond to the thermal energies of the nuclei at the stellar temperatures of interest. The reaction rate per unit volume at the temperature, T, will be given by

$$r(T) = N_1 N_2 (1+\delta_{12})^{-1} \int_0^\infty \sigma(v) \cdot v \cdot \Phi(v, T)\, dv \equiv N_1 N_2 (1+\delta_{12})^{-1} \langle \sigma v \rangle,$$

where the N's are number densities of the reacting nuclei, $\sigma(v)$ is the reaction cross section at a relative velocity, v, and $\Phi(v, T)$ is a normalized velocity distribution for the reacting nuclei at the temperature, T. For the usual case in which each nuclear species is thermalized and constitutes an ideal, nonrelativistic, Maxwellian gas, it can be shown that the velocity distribution in the center-of-mass system is also Maxwellian, so that

$$\Phi(v, T) = 4\pi v^2 \left(\frac{\mu}{2\pi kT}\right)^{3/2} \exp\left(\frac{-\mu v^2}{2kT}\right),$$

where μ is the reduced mass, $\mu = M_1 M_2/(M_1 + M_2)$. To determine the relevant energies at which to evaluate the nuclear reaction cross sections, one must examine the form of the integrand,

$$[\sigma(v) \cdot v \cdot \Phi(v, T)]$$

to find out at what energies the largest contributions to the integral, $\langle \sigma v \rangle$, are expected for the various kinds of nuclear reactions.

Neutron induced reactions are of interest for (1) heavy-element production ($A > 56$) via the r-process and s-process neutron capture chains and (2) reactions with light nuclei in the process of explosive nucleosynthesis. In the heavy nuclei encountered in the r- and s-processes the average neutron binding energy is $\sim$8 MeV, and at these excitation energies in the compound nucleus the level spacing is only $\sim$1 keV or less. With no Coulomb barrier, the neutron widths for these resonances become larger than their spacing for neutron energies greater than a few keV, and it becomes a very difficult experimental problem to resolve and study the individual resonances under these circumstances. Instead, the normal method is to use an incident neutron beam with sufficiently poor energy resolution to average over the resonances. Although this approach loses a lot of detailed nuclear structure information, for the astrophysical problems it is really not an unreasonable procedure since the thermal velocity distribution, $\Phi(v, T)$, will average over these resonances in much the same way. This averaged cross section varies only slowly with energy so that the integral, $\langle \sigma v \rangle$, finds its largest contributions near the peak of the Maxwellian velocity distribution, $E = kT$. For the temperatures of interest for the r- and s-processes (10^7 to 5×10^9 °K) this means that the relevant neutron energies for cross section measurements cover the range 1 keV $\lesssim E_n \lesssim$ 500 keV. In fact, it turns out that to a very good approximation[7] for neutron induced reaction in this energy

range the averaged cross section can be expressed as simply proportional to $1/v$,

$$\sigma(v) = S_0/v$$

$$\langle \sigma v \rangle = \int_0^\infty \frac{S_0}{v} v \, \Phi(v, T) \, dv$$

$$= S_0 = [\sigma(v) \cdot v],$$

which is constant, independent of v within this region.

For light nuclei the level densities are not nearly as great so that the cross section for light nuclei participating in high temperature explosive nucleosynthesis[8] require the study of the individual resonances in the region from 0 to about 500 keV. The possibility of nucleosynthesis in super-massive stars in the early life of the galaxy depends in part on the measurement of such resonant cross sections, and a few of the more important of these are listed in Table I.

Below $A = 56$, measurements of the (n, γ) cross sections of the isotopes of Si, S, Ar, Ca, Ti, and Cr are needed to ascertain the extent to which the neutron-rich isotopes of these elements may have resulted from *s*-process capture on their $A = 4n$ seed nuclei following Silicon burning.[9]

For heavier nuclei, it can be said in general that every nucleus in the *s*-process chain can be usefully measured, but the most important measurements are those on neutron-magic nuclei and nuclei shielded from *r*-process production. An example of this situation which is of particular importance for cosmochronological applications is shown in Fig. 1 where Os^{186} is an *s*-only nucleus (shielded from the *r*-process by the stable W^{186} (*r*-only)) while Os^{187} will also contain contributions from Re^{187} via its 4×10^{10}-year half life β-decay.[10] Some of the other more interesting areas for *s*-process studies are listed in Table II. Studies of the *r*-process and the *s*-process in reactions such as these should lead to determinations of both the temperature at which our solar system material was formed[11] and the time of the origin of these elements.[10]

TABLE I

Light-element neutron resonances of importance to explosive nucleosynthesis

Reaction	Q (MeV)	Resonances E_r (cm, keV), J^π
$Li^6(n, \gamma)\, Li^7$	7.253	222, $5/2^-$
$Be^9(n, \gamma)\, Be^{10}$	6.815	562, 3^- 733, 2^+
$B^{10}(n, \gamma)\, B^{11}$	11.456	220, $5/2^+$ or $7/2^+$ 490, $3/2^-$ or $5/2^+$
$B^{11}(n, \gamma)\, B^{12}$	3.369	18, $\leqslant 3^+$ 390, 2^+
$C^{12}(n, \gamma)\, C^{13}$	4.947	560 ?
$Be^7(n, \alpha)\, He^4$	18.991	$\sim$0, 2^- 150, 3? 320, 3^+
$C^{13}(n, \gamma)\, C^{14}$	8.176	147, 1^+ or 2^+
$N^{14}(n, \gamma)\, N^{15}$	10.835	470, 600,
$O^{16}(n, \gamma)\, O^{17}$	4.143	409, $3/2^-$
$O^{17}(n, \gamma)\, O^{18}$	8.046	160, 2^+ 233, 3^-
$O^{18}(n, \gamma)\, O^{19}$	3.956	150,
$Ne^{20}(n, \gamma)\, Ne^{21}$	6.760	540,
$O^{17}(n, \alpha)\, C^{14}$	1.819	160, 2^+ 233, 3^-

TABLE II

Neutron capture cross sections needed for clarification of *s*-process

Nuclei	Remarks
All Fe, Co, Ni, Cu isotopes	Required for Cu-Ni synthesis.
Ge^{70}, Ge^{72}, Ge^{73}, Ge^{74}	Reverse trend in σN but discrepancy in Ge^{74} measurements.
Cd^{106} to Cd^{116}	Eight isotopes, five *s*-process. Similar to tin.
Ba^{130} to Ba^{138}	Current *estimates* for σ yield reverse trend in σN.
Os^{186}, Os^{187}, Os^{188}	Currest estimates yield high σN. Cosmochronology: $Re^{187} \rightarrow Os^{187}$.
Pb^{208}, Pb^{207}, Pb^{206}, Pb^{204}	Present error ($\sigma_{208} = 3 \pm \frac{1}{2}$) leaves cosmochronology uncertain.
Sr^{86}, Sr^{87}	Possible cosmochronology: $Rb^{87} \rightarrow Sr^{87}$.
N = 50: Sr^{88}, Y^{89}, Zr^{90}, Kr^{86}	Precipice near A = 88–90; possible *s*-source of Kr^{86}.
N = 82: Ba^{138}, La^{139}, Ce^{140}, Pr^{141} Nd^{142}	Precipice near A = 138–142.
All shielded *s* nuclei	σN_s curve, element abundances.

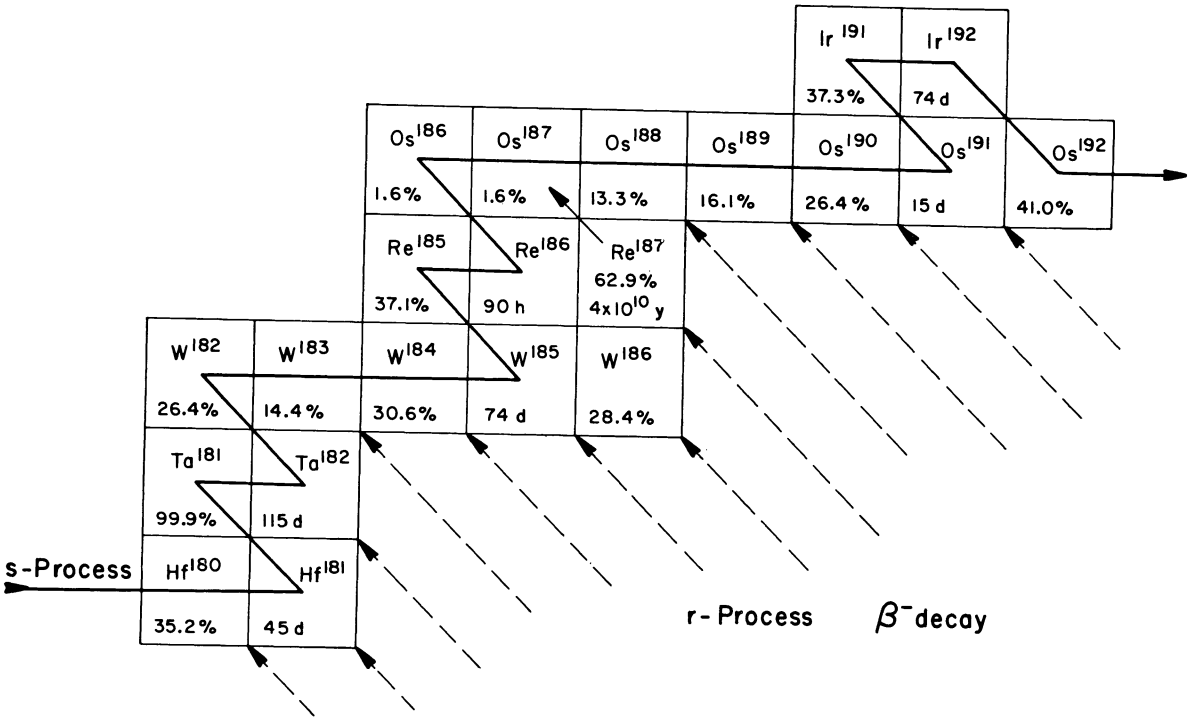

FIG. 1. *S*-process neutron-capture path and *r*-process β-decays for nuclei with $180 \leqslant A \leqslant 192$.

The prospective experimentalist who is contemplating such a program is cautioned, however, that it involves many very challenging experimental problems such as the production of collimated neutron beams of reasonable energy resolution in the energy range from 1 to 100 keV, and the development of accurate and sensitive counting techniques. An example of the type of experimental apparatus which is required for such measurements is provided by the continuing project carried out by Macklin and Gibbons[12] at Oak Ridge using a 3-MV pulsed proton beam incident on a Li^7 target as the neutron source together with gamma-ray spectrometers, such as a Moxon-Rae[13] detector, and a time-of-flight system.

For charged-particle induced reactions some of the problems associated with the incident beam and the detection of reaction products may become slightly simpler, but the interpretation and the application of these measurements to astrophysical calculations become much more difficult because of the inhibiting effect of the Coulomb barrier. At energies below $\sim$1 MeV, the energy dependence of charged-particle reaction cross sections (perhaps modulated by resonance structure) will be dominated by the Coulomb-barrier penetrability term $\exp(-2\pi Z_1 Z_2 e^2/\hbar v)$, and the $1/E$ dependence of the square of the deBroglie wavelength. Hence the nonresonant cross section is often expressed as

$$\sigma(E) = S(E)E^{-1}\exp(-2\pi Z_1 Z_2 e^2/\hbar v),$$

where $S(E)$ is then reasonably energy independent as shown in Fig. 2 for the $He^3(\alpha,\gamma)Be^7$ reaction.[14,15] In this case the integral, $\langle \sigma v \rangle$, can be re-expressed as

$$\begin{aligned}\langle \sigma v \rangle &= \int_0^\infty \sigma(v)\cdot v \cdot \Phi(v,T)\,dv \\ &= \int_0^\infty S(E)E^{-1}\exp(-b/E^{1/2})\sqrt{\frac{2E}{\mu}}\frac{2}{\sqrt{\pi}}\frac{E^{1/2}}{(kT)^{3/2}} \\ &\qquad \cdot \exp(-E/kT)\,dE \\ &= \sqrt{\frac{8}{\pi\mu k^3 T^3}}\int_0^\infty S(E)\exp[-b/E^{1/2}-E/kT]\,dE\end{aligned}$$

where

$$\begin{aligned} b &\equiv [2\pi Z_1 Z_2 e^2/\hbar(2/\mu)^{1/2}] \\ &= 31.28 Z_1 Z_2 A^{1/2}\,\mathrm{keV}^{1/2}\end{aligned}$$

and where A is the reduced atomic mass, $A = A_1 A_2/(A_1 + A_2)$. Assuming $S(E)$ is reasonably constant (e.g. Fig. 2), the integral now contains the

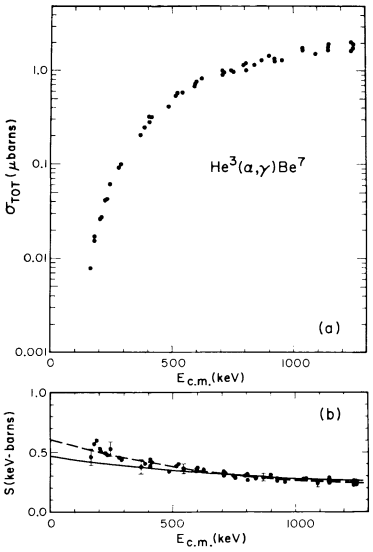

FIG. 2. The energy dependence of (a) the total cross section and (b) the S-factor for the $He^3(\alpha,\gamma)Be^7$ reaction.[14,15] The significance of the solid and dashed lines in (b) are discussed in the text.

product of 2 rapidly varying exponentials as shown in Fig. 3, and the maximum contribution to the integral no longer occurs at $E \approx kt$ (as for the neutron case) but at the maximum for the product of these two exponentials,

$$E_0 = (bkT)^{3/2}$$
$$= 1.220(Z_1 Z_2 A T_6)^{1/3}\,\text{keV},$$

where T_6 is the temperature in millions of degrees Kelvin. The width of the peak in the integrand is given by

$$\Delta = 4(E_0 kT/3)^{1/2}$$
$$= 0.749(Z_1^2 Z_2^2 A T_6^5)^{1/6}\,\text{keV}.$$

For the $He^3(\alpha,\gamma)Be^7$ reaction which is one link in the *pp*-chain for converting hydrogen into helium at temperatures of $\sim 15 \times 10^6$ °K in our sun,

$$kT = 1.3\ \text{keV}$$
$$E_0 = 14\ \text{keV}$$
$$\Delta = 12\ \text{keV}.$$

In the data shown in Fig. 2, however, it is clear that because of the inhibition of the Coulomb barrier it has not been possible to measure the cross section for this reaction at center-of-mass energies below 164 keV where $\sigma_{tot} = 7.8 \times 10^{-9}$ barns. Therefore, any study of the role of this reaction in stars like

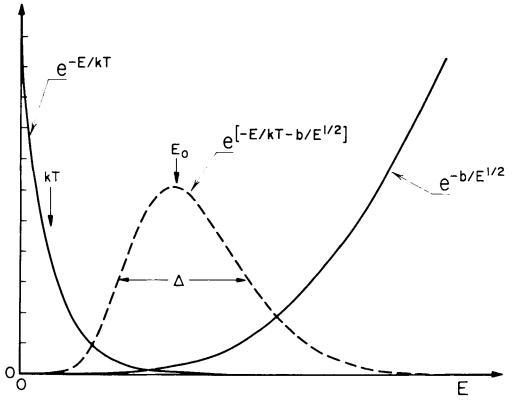

FIG. 3. The dominant energy dependent terms in the evaluation of $\langle\sigma v\rangle$ for charged-particle reactions.

our sun at temperatures of the order of 15×10^6 °K ($E_0 = 14$ keV) must depend on an extrapolation from the experimentally accessible region down into the astrophysically interesting region. ($S(E)$ with its relatively weak energy dependence is obviously much more suited for such an extrapolation than is the cross section, $\sigma(E)$.) The details of how such an extrapolation is made are discussed below. Although we have used the $He^3(\alpha,\gamma)Be^7$ reaction as an example here because of its nonresonant character, these Coulomb-barrier problems and associated extrapolations are a general characteristic of almost all charged-particle induced nuclear reactions of interest in astrophysics.

In addition to the nonresonant cross sections, we must also be concerned with nuclear reaction resonances whose contributions must also be included in the evaluation of the integral, $\langle\sigma v\rangle$. Resonances will obviously be important when they occur in the region of astrophysical interest ($E_{Res} \approx E_0$), but even when they are well removed from E_0 they may also be of importance because of the contributions to σ_{tot} from the wings of such resonances. An example of the latter case is seen in the data for the $C^{12}(p,\gamma)N^{13}$ reaction[16] in Figs. 4 and 5. In this case, at $E_0 = 34$ keV (25×10^6 °K) the tail of the 460-keV resonance contributes roughly half of the total cross section.

The problem of extrapolating from the experimental measurements to the effective thermal energy, E_0, can be handled in two ways. One method which often must be used involves empirical extrapolation on the basis of some fit (e.g. a linear or quadratic least-squares analysis) of the higher energy data points and the necessary assumption

that this measured behavior continues unchanged into the astrophysical region. In some cases, however, the extrapolation can be made on somewhat firmer ground if a model exists for the reaction mechanism from which the energy dependence of the cross section can be predicted.[17] The solid curve in Fig. 2(b) is the result of such a calculation for the $He^3(\alpha, \gamma)Be^7$ reaction based on a direct-capture mechanism which has been normalized to measurements covering the energy range

$$181 \leqslant E_{cm} \leqslant 2500 \text{ keV}.$$

The problem which exists with this technique is one of determining over what energy range this normalization should be carried out; over what energy range, if any, it is valid to consider only this reaction mechanism. In this particular case, if the normalization is made to only the low energy points, $E_{cm} \leqslant 625$ keV, then the value for S in the astrophysical region is roughly 10% higher. [The dashed line in Fig. 2(b) is a quadratic, least-squares fit of the data for $E_{cm} \leqslant 1250$ keV.]

The reaction $He^3(He^3, 2p)He^4$ is a good example of a reaction mechanism changing for a non-

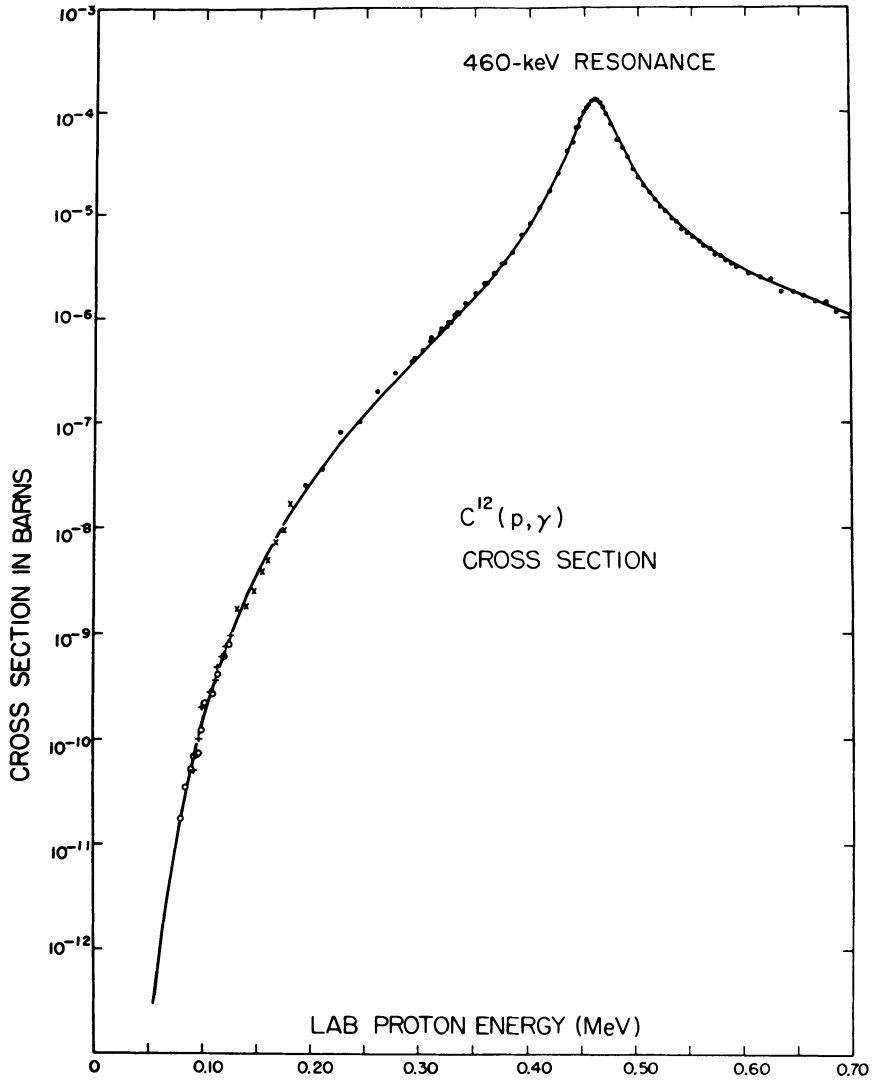

FIG. 4. The energy dependence of the cross section for the $C^{12}(p, \gamma)N^{13}$ reaction,[16] including the effects of the 460-keV resonance corresponding to the first excited state in N^{13} at 2.365 MeV. The solid line is a fit to the data of the form $\sigma_{TOT} = \sigma_{RES}[1 + A(E_R - E)]^2$.

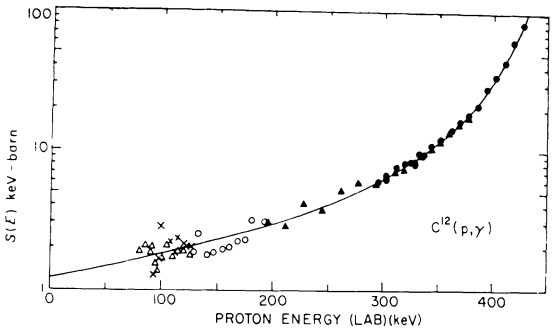

FIG. 5. The energy dependence of the S-factor for the $C^{12}(p, \gamma)N^{13}$ reaction.[16] (See Fig. 4.)

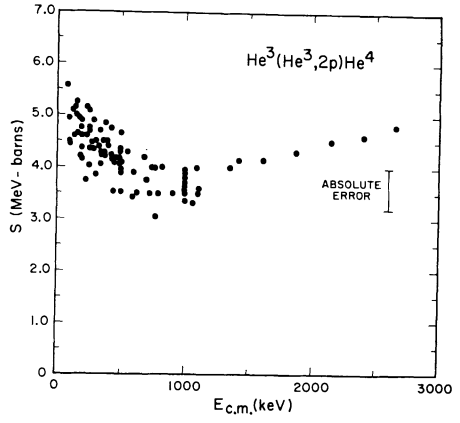

FIG. 6. The energy dependence of the S-factor for the $He^3(He^3, 2p)He^4$ reaction,[18–20] indicating a possible change in the reaction mechanism at $E_{c.m.} \approx 1$ MeV.

resonant reason. The cross-section factor, $S(E)$, measured by three independent experiments[18–20] is shown in Fig. 6. Above 1 MeV, a two-step process involving $Li^5 + p$ as an intermediate state dominates the reaction, and S is observed to decrease with decreasing energy. Below 1 MeV, however, this two-step process decreases greatly in importance, and S begins to increase with decreasing energy. (May and Clayton[21] have suggested that the low-energy reaction mechanism may be a direct tunneling of a neutron from one He^3 to the other.) In any case, it appears likely that near 1 MeV a transition occurs between two different three-body reaction mechanisms, and we cannot make a confident extrapolation of $S(E)$ to astrophysical energies without an understanding of those reaction mechanisms and the transition which occurs.

The solid lines in Figs. 4 and 5 are theoretical fits to the measured cross sections on the basis of the Breit-Wigner single-level formula for the resonance combined with a semi-empirical fit to a term of the form

$$\sigma_{\text{tot}} = \sigma_{\text{Res}}[1 + A(E_R - E)]^2$$

to take into account interference between the nonresonant cross section and the tail of the resonance.[16]

Resonances which occur in the energy range of astrophysical interest, $E_R \approx E_0$, present quite a different set of problems from those discussed in connection with Figs. 4 and 5. Because of the inhibition of the Coulomb barrier the properties of such resonances can rarely be measured directly in the reaction of interest but must be inferred from studies of the corresponding nuclear excited states via other reactions which will hopefully provide the necessary information about the exact energy, width, spin-parity, and decay modes of the state.

In the $N^{14}(p, \gamma)O^{15}$ reaction the (p, γ) threshold lies at an excitation energy of 7293 keV. Two preliminary experiments located an excited state on O^{15} at 7284 ± 7 keV[22] and 7285 ± 10 keV[23], presenting a real possibility for a resonance at stellar energies which could increase the importance of the CN cycle in the sun and severely affect the expected N^{14}/N^{15} abundance ratio. Therefore, two very accurate subsequent measurements were necessary to establish the level's excitation at 7271 ± 2 keV[24] and 7276 ± 1 keV[25] and to establish its spin-parity as $7/2^{(+)}$, requiring d-wave proton capture.[24] Because of this location, 17 to 22 keV below threshold, and because of the d-wave centrifugal barrier it is now concluded that this level does not have any astrophysical significance. Some other examples of this kind of problem include the $3He^4 \rightarrow C^{12}$ reaction,[26] the $C^{13}(p, \gamma)N^{14}$ reaction,[27] the $C^{12}(\alpha, \gamma)O^{16}$ reaction,[28] the $N^{14}(\alpha, \gamma)F^{18}$ reaction.[29] (For the $C^{12}(\alpha, \gamma)$ and the $N^{14}(\alpha, \gamma)$ reactions the problem is not yet solved.)

In carrying out nuclear physics experiments for astrophysical applications, two of the primary requirements for such measurements are the need for precise energy determinations and the need for accurate, absolute, total cross sections. Accurate energy measurements are required for determining the role of nuclear levels as possible astrophysical resonances as discussed in the preceding paragraph and are also necessary for nonresonant measurements because of the very steep energy variation of the Coulomb barrier. In the $N^{14}(\alpha, \gamma)F^{18}$ reaction, for example, a 1% change

in the α-particle energy from 1000 to 990 keV would cause a 15% reduction in the nonresonant direct-capture cross section.

For the accelerator beam this requirement is normally met with either an electrostatic or magnetic analyzer, but consideration must also be given to the related problems of energy losses[30-32] in the target (and in the entrance foil for a gas target), the possible accumulation of oil vapour and other contaminants on the target surface which degrade the beam energy before it reaches the target material, etc. (In connection with any discussion about possible choices of target materials, mention should be made of the recirculating, differentially-pumped, gas target system[20] which allows the use of rare, expensive gases in a windowless gas target. Furthermore, while virtually all stable isotopes are now available in highly enriched forms, it should be emphasized that experiments need not be restricted to stable isotopes. There are many interesting and important measurements to be made with radioactive targets such as Be^7, Be^{10}, C^{14}, Ar^{37}, and Ti^{44}, and a small laboratory with a strong radiochemistry background might well consider that the development of such a target could be as important a stimulus for the creation of an active research program as the acquisition of a lot of complicated and expensive hardware for use in studying more mundane nuclei.)

For nuclear reaction products, accurate energy determinations can be obtained for charged particles using magnetic spectrographs or energy sensitive detectors such as Si(SB) diodes which are calibrated against other reaction products of known energy. For neutrons the best energy precision is provided by time-of-flight systems using a standard 'long counter' or a fast-rise-time organic scintillator such as Pilot-B. Semi-conductor devices can also be used for neutrons by sandwiching a thin Li^6 or B^{10} layer between two Si(SB) devices and detecting the (n, α) reaction products,[33] or by detecting the $Si(n, \alpha)$ and $Si(n, p)$ reactions in the volume of the detector itself.[34] Using the latter technique, on the basis of comparisons with groups of known energies, energies have been obtained for unknown neutron groups with precisions of ± 5 keV to ± 15 keV, comparable with the precision of time-of-flight systems. For γ-rays the most precise energy measurements are now provided by Ge(Li) detectors; in fact, these detectors now often provide the most accurate way for determining the excitation energy of a γ-emitting nuclear level. A convenient set of calibration lines with energies covering the range from 2.3 to 7.1 MeV have been measured by Chasman *et al.*[35] (This was the technique used in Ref. 25 to obtain a precise measurement of the excitation energy of the 7274-keV level in O^{15} discussed earlier.)

Another interesting technique that has been suggested to take advantage of the high resolution of the Ge(Li) detectors is the measurement of radiative-capture excitation functions using a thick target and one fixed bombarding energy. The measured thick target γ-ray spectrum, after correction for energy variations in target stopping power and detector efficiency becomes a plot of the capture cross section vs. energy. The effective bombarding-energy resolution is determined by the resolution of the detector, and is independent of accelerator stability and energy spread and of target thickness uniformity. This method should be useful in cases where the capture γ-ray cascade is simple, as in the case of the $C^{12}(p, \gamma)N^{13}$ reaction at low energies.[36]

For absolute cross section measurements, accurate beam-current integration is required with adequate electrostatic or magnetic suppression of secondary electrons[37] and with account taken of the various equilibrium charge-state abundances for heavy ion beams.[38] For cases where a significant fraction of the beam may be neutral or where it is not possible to make an accurate or meaningful charge integration because of charge changing collisions before the beam enters the Faraday cup, Winkler and Dwarakanath[20] have devised a method for ignoring the charge of the incident beam and instead simply measuring the beam *power* using a balanced calorimeter. This method treats particles of all charge states equally, and when combined with an accurate energy measurement it gives an accurate determination of the number of incident particles corresponding to a given 'run'.

In addition to beam integration, in order to extract absolute cross sections, accurate measurements must also be available for the target thickness and the detector efficiency. Target thickness can be determined from excitation function measurements across a narrow resonance ($\Gamma_R \lesssim \Delta E_{tgt}$), from the measurement of the energy loss for transmitted α-particles[39] (for thin targets which are either self-supporting or mounted on thin backings of known thickness), and from back-angle target-profile measurements with a magnetic spectrometer[40] (for targets mounted on thick, heaving backings). For gas targets the thickness can be

computed by knowing the gas temperature and pressure, but consideration must also be given to local beam-heating effects[41] which may raise the gas temperature along the beam path by as much as 50 °C. (For charged-particle reaction products the measurement of a Rutherford scattering cross section often provides a good check on the combination of beam integration, target thickness and detector efficiency determinations.)

Although the total efficiency for γ-ray detection by a NaI(Tl) crystal (including the photoelectric, Compton and pair-production interactions) can be calculated from knowledge of the target-detector geometry and the photon absorption cross sections tabulated by Grodstein[42] and by Plechaty and Terrall,[43] this 'ideal' efficiency must be modified when utilized to extract absolute cross sections from 'real' γ-ray spectra to take into account the following considerations:

(1) attenuation of the γ-ray flux by any materials between the target and the detector;

(2) modification of the γ-ray spectrum by absorption and scattering by near-by material (this means that usually only the full-energy peak of the NaI(Tl) response function can be used and requires the measurement of the ratio of total efficiency to the efficiency of the full-energy peak[44]);

(3) effects of coincident summing of members of a cascade transition;

(4) separation of a complex spectrum into the response functions of several different monoenergetic γ-rays[44,45] as seen in Figs. 7 and 8 from an application to the $He^3(\alpha, \gamma)Be^7$ reaction[14]; etc.

For Ge(Li) γ-ray detectors similar considerations apply; however, because of the high resolution of these detectors usually only the full-energy or single-escape or double-escape peaks in the spectrum are analyzed,[46] and usually the efficiencies for these peaks are determined empirically using calibrated sources.

In many cases in nuclear astrophysics experiments, the required information involves the determination of total cross sections. For instance, in a measurement of the rate of the $C^{13}(p, \gamma)N^{14}$ reaction as part of the CNO cycle, it is not of any particular importance to know whether the capture occurs directly to the N^{14} ground state or via a cascade of γ-rays through the excited states of N^{14}; what is important to know is how many $N^{14}_{g.s.}$ nuclei are eventually formed. This total cross-section information must normally be collected first from an integration over the angular distribution of each

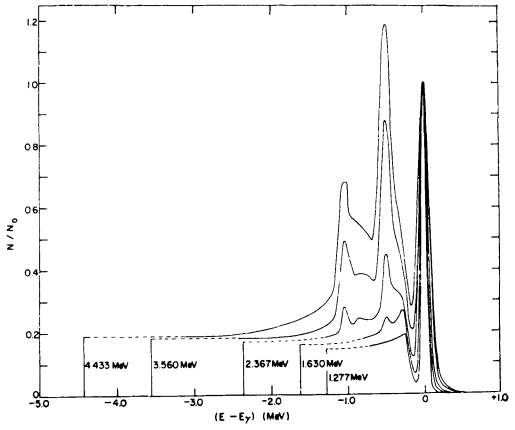

FIG. 7. The line-shape response calibration of a 3″ × 3″ NaI(Tl) crystal as measured experimentally using various nuclear reactions to produce the monoenergetic γ-rays. The γ-ray energy is indicated at the low-energy end of each function. From such a calibration, it is possible to interpolate the line-shape response at any intermediate energy.

of the reaction products and then from a summation over the contributions of all the various, relevant decay channels. In cases where only a very few decay channels are involved, these integration and summation techniques are feasible but cumbersome. For cases, such as the $Al^{27}(p, \gamma)Si^{28}$ reaction, where the number of decay channels is more than just a very few, this method becomes so cumbersome as to be no longer practical, and other means must be found.

One technique, which can be feasible whenever the residual nucleus is unstable, involves simply using the *specific, residual radioactivity* (together with the usual lifetime and efficiency corrections) as a measure of the total cross section, as in the case of the $Be^7(p, \gamma)B^8$ reaction[47,48] or the $N^{14}(\alpha, \gamma)F^{18}$ reaction.[29] For measuring very small cross sections this technique has additional advantages in terms of measuring the delayed activity at times or places removed from the intense, prompt, beam-induced radiations and oftentimes in better geometry or with better shielding than would have been practical at the target chamber location.

A second technique which has been used for measuring total γ-ray cross sections involves the use of a Moxon-Ray detector.[13] These detectors consist of a thick, low-z (e.g. graphite) gamma-to-electron converter together with a thin ($\approx$0.020-in.) plastic scintillator for detecting the electrons, and on the basis of this these detectors have an efficiency which is a linear function of the γ-ray energy. The

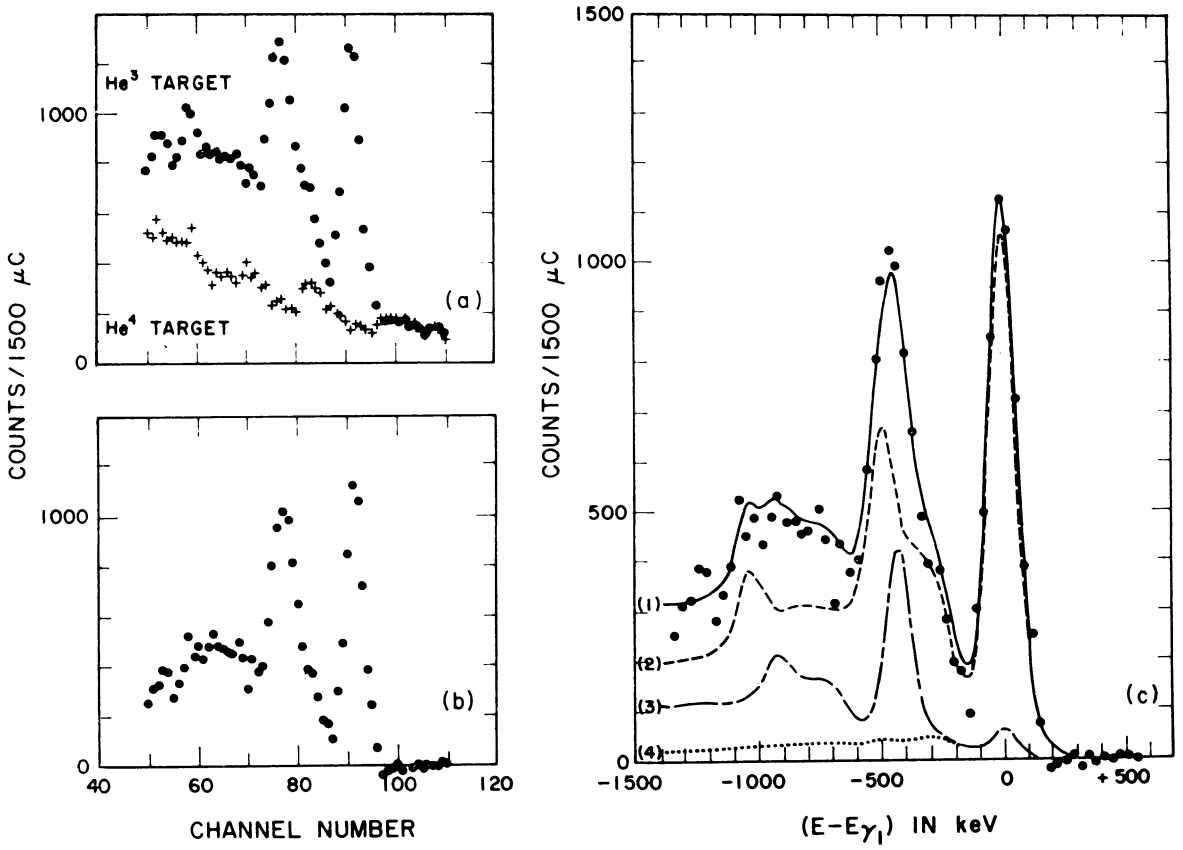

FIG. 8. Graphical representation of the data reduction and analysis for the case of the $He^3(\alpha, \gamma)Be^7$ reaction at E_{cm} = 1248 keV. (a) The dots represent the raw NaI(Tl) spectrum obtained using He^3 as the target gas while the crosses represent the raw spectrum obtained under identical conditions using He^4 in the target chamber; (b) The dots represent the net $He^3(\alpha, \gamma)Be^7$ γ-ray spectrum obtained by subtracting the He^4 spectrum from the He^3 spectrum in (a); (c) The net experimental $He^3(\alpha, \gamma)Be^7$ spectrum is represented by the dots. Curve (1) is the least-squares fit to the net spectrum obtained by varying the normalizations of curves (2) and (3) where (2) is the response function for the crossover transition and (3) is the response function for the cascade transition including the effects of coincident summing. Curve (4) is just the contribution of such summing to the cascade response function.

efficiency for 'detecting' a γ-ray cascade is simply the sum of the efficiencies for detecting each of the members of the cascade (provided your geometry is good enough to eliminate the problem of summing due to the coincident detection of two or more members of the cascade). Therefore, the Moxon-Rae detector, whose efficiency is a linear function of γ-ray energy, has the *same* efficiency for detecting each of the different cascades from a particular initial state, regardless of the number of γ-rays involved or their individual energies, i.e. since

$$E_{\text{cascade}} = \sum_i E_{\gamma_i} = E_{\gamma 0} \quad \text{and} \quad \eta_i \propto E_{\gamma_i}$$

$$\therefore \quad \eta_{\text{cascade}} = \sum_i \eta_i = \eta_0 .$$

The thin plastic scintillators used in these detectors have the further advantages that their small volume makes them insensitive to direct γ-ray or neutron detection and that their fast response times ($\approx$2 nsec) enable them to be used for (n, γ) experiments with pulsed-beam and time-of-flight techniques to separate the (n, γ) events from the intense prompt radiation produced by the primary beam in the target being used to generate the neutrons.

Other alternatives for obtaining total cross-section information include the use of large, well-type detectors to surround the target as completely as possible, thereby integrating over any angular distribution effects, or the sum-geometry technique

of Lyons *et al.*,[49] which utilizes two large NaI(Tl) crystals to surround the target and, with their outputs summed, to act like a large, well-type crystal. In analyzing the spectra (including a large summing contribution) obtained in this way, Lyons *et al.*[49] have found empirically that for a discriminator setting of $\approx 0.33 \times E_{\gamma 0}$ the efficiencies for detecting cascades involving one, two or three γ-rays are very nearly the same, $\pm 5\%$, allowing one to ignore the problem of branching ratios as well as the problem of angular distribution for such detectors.

In experimental nuclear astrophysics, the problems associated with determining *absolute*, *total* cross sections are almost always compounded by the fact that these cross sections must be measured at energies far below the Coulomb barrier where the interesting yields become vanishingly small. These low yields make the reduction or elimination of backgrounds one of the most serious problems in experimental nuclear astrophysics, especially for γ-ray experiments where the large volume of the detectors make them much more sensitive to ambient background radiations such as cosmic rays, K^{40}, Zn^{65}, ThC″, and the radiation associated with the operation of the accelerator.

The brute-force way of handling this problem involves the use of massive shielding around the detector, but in this case one must be aware of possible spectrum changes caused by the scattering of radiation into the detector by this shielding as discussed earlier for γ-ray experiments. Other fairly obvious procedures include the use of high-intensity beams, the detection of delayed activities as discussed earlier in this section, and the placing of the detector as close as possible to the target. (In most cases the angular resolution gained by 'good' geometry is not relevant to the astrophysical interest in the reaction.) In this 'poor' geometry, however, added care must be taken to define accurately and maintain the position of the beam on the target relative to the detector since a small absolute change in this position can represent an important relative change at such close distances and thus result in a substantial change in the detector efficiency.

Additional precautions relevant to background reduction should include target purity and the cleanliness of the vacuum systems as related, for example, to carbon contamination and the $C^{13}(\alpha, n)O^{16}$ reaction discussed earlier. For low-yield experiments attention must also be given to the problems of ion-source cleanliness. A good electrostatic or magnetic-beam analyzer will normally remove any contaminating component from the beam before it reaches the target; however, the additional background produced by the elimination of this contaminant beam (for instance, deuterons) on a set of defining slits or apertures can be devastating to a low-yield reaction such as (α, γ). For this reason, before starting such an experiment it may often be necessary to run the ion source for a day or more simply to cook out any residual gases from the previous operations.

Finally, once the background level has been reduced as much as practical, for low-yield experiments it is just as important to obtain accurate measurements of the various components of the remaining background as it is to obtain measurements of the radiations from the reaction of interest. Techniques for these background measurements include the use of data obtained at energies very slightly removed from narrow resonances and the use of 'dummy' targets which are chemically similar to the 'real' targets but in which the element or isotope of interest is absent or at least significantly reduced.

Although some laboratories already have active experimental programs under way in nuclear astrophysics, there still remain a large number of unanswered problems which could be successfully attacked by any group which has access to a low-energy accelerator and which is interested in initiating such a program. For instance, in the basic hydrogen-burning reactions, $4H^1 \rightarrow He^4$, the following problems are still of interest:

(1) a precise, absolute cross section measurement of the $Li^7(d, p)Li^8$ reaction at the 770-keV resonance (All $Be^7(p, \gamma)B^8$ data are normalized to this cross section for which two equally accurate values exist, 176 ± 15 mb[47] and 211 ± 15 mb[48]);

(2) an absolute cross section measurement of the $Li^7(n, \gamma)Li^8$ reaction, for use in calculations[17] dealing with the mirror reaction, $Be^7(p, \gamma)B^8$;

(3) further study of the 5.60 and 5.66-MeV levels in F^{18} and their influence as low-lying resonances in the $O^{17}(p, \alpha)N^{14}$ reaction as part of the CNO bicycle[50];

(4) many reactions in the Ne-Na cycle,[51,52] etc.

In the helium-burning reaction, $3He^4 \rightarrow C^{12}$, measurements of the radiative width of the 7.65 MeV state[26] should be supplemented by an accurate measurement of its energy. Present Q-value measurements from the reactions

$$B^{12}(\beta^-\bar{\nu})C^{12*}(\alpha)Be^8, \quad B^{10}(He^3, p)C^{12*}$$

and

$$N^{14}(d, \alpha)C^{12*}$$

TABLE III

Reactions relevant for nuclear astrophysics

Reaction	Application (temperature)	Reference
$H^1(p, \beta^+\nu)D^2$	hydrogen burning ($1<T_6<20$)	a,b,c
$D^2(p, \gamma)He^3$	surface convection ($0.1<T_6<5$)	a,b,d,w,y
	explosive nucl. ($T_9<5$)	h
$D^2(d, p)T^3$	explosive nucl. ($T_9<10$)	h
$T^3(p, \gamma)He^4$	explosive nucl. ($T_9<10$)	h
$T^3(\alpha, \gamma)Li^7$	explosive nucl. ($T_9<10$)	h,x
$He^3(p, \beta^+\nu)He^4$	hydrogen burning ($1<T_6<20$)	b
$He^3(d, p)He^4$	early hydrogen burning (probably unimportant)	b
$He^3(He^3, \gamma)Be^6$	explosive nucleosynthesis ($T_9<5$)	h
	hydrogen burning	aa
$He^3(He^3, 2p)He^4$	hydrogen burning, ν astron. ($5<T_6<20$)	a.b.d.e.f.i
$He^3(\alpha, \gamma)Be^7$	hydrogen burning, ν astron. ($5<T_6<20$)	a,b,d,y,z
	explosive nucl. ($T_9<10$)	h
$He^4(d, \gamma)Li^6$	explosive nucl.	h
$He^4(\alpha, \alpha)He^4$	helium burning	bb,cc
$Li^6(p, \gamma)Be^7$	explosive nucl.	h
$Li^6(p, \alpha)He^3$	surface convection ($T_6<2$)	j
	explosive nucl. ($T_9<5$)	g,h
$Li^6(\alpha, \gamma)B^{10}$	explosive nucl. ($T_9<4$)	h
$Li^7(p, \alpha)He^4$	hydrogen burning ($5<T_6<20$)	a,b,g
	surface convection ($T_6<2$)	j
	explosive nucl. ($T_9<5$)	h
$Li^7(\alpha, \gamma)B^{11}$	explosive nucl. ($T_9<3$)	h
$Be^7(p, \gamma)B^8$	hydrogen burning, ν astron. ($5<T_6<20$)	a,b,d,g,l
	explosive nucl. ($T_9<10$)	h
$Be^7(\alpha, \gamma)C^{11}$	explosive nucl. ($T_9<2$)	h
$Be^8(\alpha)He^4$	helium burning	bb,cc
$Be^8(\alpha, \gamma)C^{12}$	helium burning, $3\alpha(0.1<T_9<10)$	g,k
$Be^9(p, \gamma)B^{10}$	explosive nucl. ($T_9<10$)	h
$Be^9(p, \alpha)Li^6$	explosive nucl. ($T_9<10$) surface convection	h,j
$Be^9(p, d)Be^8$	explosive nucl. ($T_9<10$)	h
$Be^9(\alpha, n)C^{12}$	explosive nucl. ($T_9<10$)	h,ii
$Be^{10}(p, \gamma)B^{11}$	explosive nucl.	h
$Be^{10}(p, \alpha)Li^7$	explosive nucl.	h
$Be^{10}(\alpha, n)C^{13}$	explosive nucl.	h
$B^{10}(p, \gamma)C^{11}$	explosive ($5<T_9<10$)	h
$B^{10}(p, \alpha)Be^7$	explosive ($T_9<5$), surface convection	h,j
$B^{10}(\alpha, n)N^{13}$	explosive	h
$B^{10}(\alpha, p)C^{13}$	explosive	h
$B^{11}(p, \gamma)C^{12}$	explosive ($T_9<10$), surface convection	h.j
$B^{11}(p, \alpha)Be^8$	explosive ($T_9<10$), surface convection	h,j
$B^{11}(\alpha, n)N^{14}$	explosive ($T_9<10$), surface convection	h
$B^{11}(\alpha, p)C^{14}$	explosive ($T_9<10$), surface convection	h
$C^{12}(p, \gamma)N^{13}$	CNO ($T_6<100$)	a,g,m,dd
	carbon burning ($0.6<T_9<5$)	n
$C^{12}(n, \gamma)C^{13}$	carbon burning	n
$N^{13}(p, \gamma)O^{14}$	CNO ($T_6>100$)	g,m
$C^{13}(p, \gamma)N^{14}$	CNO ($T_6<100$)	a,g,m,ee
	carbon burning ($0.6<T_9<5$)	n
$N^{14}(p, \gamma)O^{15}$	CNO ($T_6<100$)	a,g,m,o,ff
$N^{15}(p, \gamma)O^{16}$	CNO	a,g,m,gg
$N^{15}(p, \alpha)C^{12}$	CNO	a,g,m
$O^{16}(p, \gamma)F^{17}$	CNO	a,g,m,hh
	carbon and oxygen burning ($T_9<5$)	n
$O^{16}(n, \gamma)O^{17}$	carbon burning ($1<T_9<5$)	n
$O^{17}(p, \alpha)N^{14}$	CNO, carbon and oxygen burning	a,g,m,n
$C^{12}(\alpha, \gamma)O^{16}$	helium burning ($1<T_8<5$)	a,g,p,pp
	carbon burning ($0.6<T_9<5$)	g,n,pp
	silicon burning ($3<T_9<6$)	g,q,pp
$C^{13}(\alpha, n)O^{16}$	helium burning ($0.7<T_8<3$), n's	a,g,r,ii
	carbon burning ($0.6<T_9<5$)	n, ii
	thermal instability and mixing	u,v
$N^{13}(\alpha, p)O^{16}$	carbon burning ($1<T_9<5$)	n
$N^{13}(n, p)C^{13}$	carbon burning ($1<T_9<5$)	n
$N^{14}(\alpha, \gamma)F^{18}$	helium burning ($0.7<T_8<2$)	g,s,kk
	carbon burning ($T_9<5$)	n
$O^{16}(\alpha, \gamma)Ne^{20}$	helium burning ($1<T_8<5$)	a,g,p
	carbon and oxygen burning ($1<T_9<5$)	n
	silicon burning ($3<T_9<6$)	q
$O^{16}(n, \gamma)O^{17}$	carbon and oxygen burning ($1<T_9<5$)	n
$O^{17}(\alpha, n)Ne^{20}$	helium burning, n's	a.g.r
	carbon and oxygen burning ($1<T_9<5$)	n
$Ne^{20}(\alpha, \gamma)Mg^{24}$	helium burning ($1<T_8<5$)	a,g,p
	carbon and oxygen burning ($1<T_9<5$)	n
	silicon burning ($3<T_9<6$)	q
$O^{17}(p, \alpha)N^{15}$	helium burning with mixing ($0.6<T_8<2$)	u
	carbon burning	n
$O^{18}(\alpha, \gamma)Ne^{22}$	helium burning ($1<T_8<3$)	a,g,r,s
$O^{18}(\alpha, n)Ne^{21}$	helium burning ($T_8\geqslant 2$), n's	r,s
$F^{18}(n, p)O^{18}$	carbon burning ($1<T_9<5$)	n
$Ne^{21}(\alpha, n)Mg^{24}$	helium burning, n's ($1<T_8<3$)	a,g,r
	carbon and oxygen burning ($T_9<5$)	n
$Ne^{22}(\alpha, n)Mg^{25}$	helium burning, n's ($T_8\lesssim 3$)	a,g,r,s,t
	carbon and oxygen burning ($T_9<5$)	n
$Ne^{22}(\alpha, \gamma)Mg^{26}$	helium burning ($1<T_8<3$)	r
	carbon and oxygen burning	n
$Ne^{20}(p, \gamma)Na^{21}$	NeNa cycle ($20<T_6<100$)	jj
	carbon and oxygen burning ($T_9<5$)	n
$Na^{21}(n, p)Ne^{21}$	carbon and oxygen burning ($T_9<5$)	n
$Ne^{21}(p, \gamma)Na^{22}$	NeNa cycle ($20<T_6<100$)	jj
	carbon and oxygen burning ($T_9<5$)	n
$Na^{22}(n, p)Ne^{22}$	carbon and oxygen burning ($T_9<5$)	n
$Ne^{22}(p, \gamma)Na^{23}$	NeNa cycle ($20<T_6<100$)	jj
	carbon and oxygen burning ($T_9<5$)	n
$Na^{23}(p, \alpha)Ne^{20}$ and $Na^{23}(p, \gamma)Mg^{24}$	NeNa cycle ($20<T_6<100$)	jj, ll
	carbon and oxygen burning ($T_9<5$)	n, ll
	silicon burning ($T_9<6$)	q, ll, mm
$Na^{23}(n, \gamma)Na^{24}$	carbon burning ($T_9<5$)	n
$Na^{23}(\alpha, p)Mg^{26}$	carbon burning ($T_9<5$)	n
$Na^{24}(p, n)Mg^{24}$	carbon burning ($T_9<5$)	n
$Mg^{23}(n, p)Na^{23}$	carbon burning ($T_9<5$)	n
$Mg^{24}(\alpha, \gamma)Si^{28}$	carbon and oxygen burning ($1<T_9<5$)	n
	silicon burning ($3<T_9<6$)	q,mm,nn
$Mg^{24}(n, \gamma)Mg^{25}$	carbon and oxygen burning ($1<T_9<5$)	n
	s-process ($0.1<T_9<2$)	oo
$Mg^{24}(p, \gamma)Al^{25}$	carbon and oxygen burning ($1<T_9<5$)	n
$Mg^{25}(p, \gamma)Al^{26}$	carbon and oxygen burning ($1<T_9<5$)	n
$Mg^{25}(\alpha, n)Si^{28}$	carbon and oxygen burning ($1<T_9<5$)	n
$Mg^{25}(n, \gamma)Mg^{26}$	carbon and oxygen burning ($1<T_9<5$)	n
	s-process ($0.1<T_9<2$)	oo
$Mg^{26}(p, \gamma)Al^{27}$	carbon and oxygen burning ($1<T_9<5$)	n
$Al^{25}(n, p)Mg^{25}$	carbon and oxygen burning ($1<T_9<5$)	n
$Al^{26}(n, p)Mg^{26}$	carbon and oxygen burning ($1<T_9<5$)	n
$Al^{27}(p, \gamma)Si^{28}$	carbon and oxygen burning ($1<T_9<5$)	n
	silicon burning ($3<T_9<6$)	q,mm,nn

Reaction	Application (temperature)	Reference
$C^{12}(C^{12}, \alpha)Ne^{20}$ $C^{12}(C^{12}, p)Na^{23}$ $C^{12}(C^{12}, n)Mg^{23}$	carbon burning ($0.6<T_9<7$)	n,rr,ss
$O^{16}(C^{12}, \alpha)Mg^{24}$ $O^{16}(C^{12}, p)Al^{27}$ $O^{16}(C^{12}, n)Si^{27}$	explosive carbon burning ($2<T_9<7$)	n,rr,tt
$O^{16}(O^{16}, \alpha)Ai^{28}$ $O^{16}(O^{16}, p)P^{31}$ $O^{16}(O^{16}, n)S^{31}$	oxygen burning ($2<T_9<7$)	qq
$O^{16}(O^{16}, Be^{8})Mg^{24}$	oxygen burning ($2<T_9<7$)	qq,uu
$Si^{28}(\alpha, \gamma)S^{32}$	oxygen burning ($1<T_9<5$)	qq
	silicon burning ($2<T_9<6$)	q,mm
$Si^{28}(p, \gamma)P^{29}$	oxygen burning ($1<T_9<5$)	qq
	silicon burning ($2<T_9<6$)	q,mm
$Si^{29}(\alpha, n)S^{32}$	oxygen burning ($1<T_9<5$)	qq
$Si^{29}(p, \gamma)P^{30}$	oxygen burning ($1<T_9<5$)	qq
$Si^{30}(\alpha, \gamma)S^{34}$ $Si^{30}(\alpha, n)S^{33}$	oxygen burning ($1<T_9<5$)	qq
$Si^{30}(p, \gamma)P^{31}$	oxygen burning ($1<T_9<5$)	qq
$P^{31}(p, \alpha)Si^{28}$ $P^{31}(p, \gamma)S^{32}$	oxygen burning ($1<T_9<5$)	qq
	silicon burning ($2<T_9<6$)	q,mm
$P^{31}(\alpha, p)S^{34}$	oxygen burning ($1<T_9<5$)	qq
	silicon burning ($2<T_9<6$)	q,mm
$P^{32}(p, n)S^{32}$	oxygen burning ($1<T_9<5$)	qq
$S^{31}(n, p)P^{31}$	oxygen burning ($1<T_9<5$)	qq
$S^{32}(\alpha, \gamma)A^{36}$	oxygen burning ($1<T_9<5$)	qq
	silicon burning ($2<T_9<6$)	q,mm
$S^{32}(p, \gamma)Cl^{33}$	oxygen burning ($1<T_9<5$)	qq
	silicon burning ($2<T_9<6$)	q,mm
$S^{32}(n, \gamma)S^{33}$	oxygen burning ($1<T_9<5$)	qq
	s-process ($0.1<T_9<3$)	oo
$S^{33}(p, \gamma)Cl^{34}$	oxygen burning ($1<T_9<5$)	qq
$S^{33}(n, \gamma)S^{34}$	oxygen burning ($1<T_9<3$)	qq
	s-process ($0.1<T_9<3$)	oo
$S^{34}(p, \gamma)Cl^{35}$	oxygen burning ($1<T_9<5$)	qq
$Cl^{35}(p, \gamma)A^{36}$	oxygen burning ($1<T_9<5$)	qq
	silicon burning ($2<T_9<6$)	q,mm
$A^{36}(\alpha, \gamma)Ca^{40}$	oxygen burning ($1<T_9<5$)	qq
	silicon burning ($2<T_9<6$)	q,mm
$Ca^{40}(\alpha, \gamma)Ti^{44}$	silicon burning ($2<T_9<6$)	q,mm
$Ti^{44}(\alpha, p)V^{47}$	silicon burning ($2<T_9<6$)	mm,vv
$Ti^{44}(n, \gamma)Ti^{45}$	silicon burning ($2<T_9<6$)	mm,vv
$Ca^{42}(\alpha, p)Sc^{45}$	silicon burning ($2<T_9<6$)	mm,vv

REFERENCES AND NOTES

a. D. D. Clayton, *Principles of Stellar Evolution and Nucleosynthesis* (McGraw-Hill Book Co., Inc., New York, 1968).

b. P. D. Parker, J. N. Bahcall, and W. A. Fowler, *Astrophys. J.*, **139,** 602 (1964).

c. J. N. Bahcall and R. M. May, *Astrophys. J.*, **152,** L17 (1968).

d. T. A. Tombrello, 'Astrophysical Problems', in *Nuclear Research with Low-Energy Accelerators*, J. B. Marion and D. M. Van Patter, eds. (Academic Press Inc., New York, 1967).

e. R. M. May and D. D. Clayton, *Astrophys. J.*, **153,** 855 (1968).

f. H. C. Winkler and M. R. Dwarakanath (to be published); A. D. Bacher and T. A. Tombrello, *Phys. Rev.* (to be published); E. W. Blackmore and J. B. Warren, *Can. J. Phys.*, **46,** 233 (1968).

g. W. A. Fowler, G. R. Caughlan, and B. A. Zimmerman, *Ann. Rev. Astron. Astrophys.*, **5,** 525 (1967).

h. R. V. Wagoner, W. A. Fowler, and F. Hoyle, *Astrophys. J.*, **148,** 3 (1967); R. V. Wagoner, *Astrophys. J. Suppl.*, No. 162 (1969); W. D. Arnett, *Astrophys. J.*, **157,** 1369 (1969); J. W. Truran and W. D. Arnett, *Astrophys. J.*, **160,** 181 (1970).

i. I. Iben, Jr., *Astrophys. J.*, **147,** 624 (1967).

j. W. A. Fowler, J. L. Greenstein, and F. Hoyle, *Geophys. J. Roy. Astron. Soc.*, **6,** 148 (1962), see Section 11, p. 185.

k. P. A. Seeger and R. W. Kavanagh, *Nucl. Phys.*, **46,** 577 (1963).

l. P. D. Parker, *Astrophys. J.*, **145,** 960 (1966); *Phys. Rev.*, **150,** 851 (1966); *Astrophys. J.*, **153,** L85 (1968); T. A. Tombrello, *Nucl. Phys.*, **71,** 459 (1965); R. W. Kavanagh, T. A. Tombrello, J. M. Mosher, and D. R. Goosman, *Bull. Am. Phys. Soc.*, **14,** 1209 (1969).

m. G. R. Caughlan and W. A. Fowler, *Astrophys. J.*, **136,** 453 (1962); **139,** 1180 (1964).

n. H. Reeves and E. E. Salpeter, *Phys. Rev.*, **116,** 1505 (1959); W. D. Arnett and J. W. Truran, *Astrophys. J.*, **157,** 339 (1969) contains a thorough list of carbon-burning reactions; see also Ref. rr.

o. D. C. Hensley, *Astrophys. J.*, **147,** 818 (1967); D. E. Alburger and E. K. Warburton, *Phys. Rev.*, **152,** 914 (1966).

p. W. Deinzer and E. E. Salpeter, *Astrophys. J.*, **140,** 499 (1964).

q. D. Bodansky, D. D. Clayton, and W. A. Fowler, *Astrophys. J. Suppl.*, No. 148 (1968); D. D. Clayton and S. E. Woosley, *Astrophys. J.*, **157,** 1381 (1969).

r. H. Reeves, *Astrophys. J.*, **146,** 447 (1966).

s. I. Iben, Jr., *Astrophys. J.*, **143,** 483 (1966).

t. J. Peters, *Astrophys. J.*, **154,** 225 (1968).

u. R. H. Sanders, *Astrophys. J.*, **150,** 971 (1968).

v. G. R. Caughlan and W. A. Fowler, *Astrophys. J.*, **139,** 1180 (1964).

w. G. M. Griffiths, M. Lal, and C. D. Scarfe, *Can. J. Phys.*, **41,** 724 (1963).

x. G. M. Griffiths, R. A. Morrow, P. J. Riley, and J. B. Warren, *Can. J. Phys.*, **39,** 1397 (1961).

y. T. A. Tombrello and P. D. Parker, *Phys. Rev.*, **131,** 2582 (1963).

z. P. D. Parker and R. W. Kavanagh, *Phys. Rev.*, **131,** 2578 (1963); K. Nagatani, M. R. Dwarakanath, and D. Ashery, *Nucl. Phys.*, **A128,** 325 (1969).

aa. W. D. Harrison, W. E. Stephens, T. A. Tombrello, and H. Winkler, *Phys. Rev.*, **160,** 752 (1967).

bb. J. Benn, E. B. Dally, H. H. Muller, R. E. Pixley, H. H. Staub, and H. Winkler, *Phys. Letters*, **20,** 43 (1966).

cc. W. Reichart, H. H. Staub, H. Stüssi, and F. Zamboni, *Phys. Lett.*, **20,** 40 (1966).

dd. R. N. Hall and W. A. Fowler, *Phys. Rev.*, **77,** 197 (1950); J. D. Seagrave, *Phys. Rev.*, **84,** 1219 (1951); D. F. Hebbard and J. L. Vogl, *Nucl. Phys.*, **21,** 652 (1960).

ee. J. D. Seagrave, *Phys. Rev.*, **85,** 197 (1952); D. F. Hebbard and J. L. Vogl, *Nucl. Phys.*, **21,** 652 (1960); R. E. Brown, *Astrophys. J.*, **137,** 338 (1963); D. D. Clayton, *Phys. Rev.*, **128,** 2254 (1962).

ff. D. F. Hebbard and G. M. Bailey, *Nucl. Phys.*, **49,** 666 (1963); D. F. Hebbard and B. Povh, *Nucl. Phys.*, **13,** 642 (1959); D. C. Hensley, *Astrophys. J.*, **147,** 818 (1967); W. A. S. Lamb and R. E. Hester, *Phys. Rev.*, **108,** 1304 (1957).

gg. D. F. Hebbard, *Nucl. Phys.*, **15,** 289 (1960).

hh. J. J. Domingo, *Nucl. Phys.*, **61,** 39 (1965); R. F. Christy and I. Duck, *Nucl. Phys.*, **24,** 89 (1961); R. E. Hester, R. E. Pixley, and W. A. S. Lamb, *Phys. Rev.*, **111,** 1604 (1958).

ii. C. N. Davids, *Astrophys. J.*, **151,** 775 (1968).

jj. J. B. Marion and W. A. Fowler, *Astrophys. J.*, **125,** 221 (1957); S. Hinds, H. Marchant, and R. Middleton, *Nucl. Phys.*, **51,** 427 (1964).

kk. P. D. Parker, *Phys. Rev.*, **173,** 1021 (1968).

ll. T. R. Fisher and W. Whaling, *Phys. Rev.*, **131,** 1723 (1963).

mm. J. W. Truran, A. G. W. Cameron, and A. Gilbert, *Can. J. Phys.*, **44,** 563 (1966).

nn. P. Lyons, *Nucl. Phys.*, **A130,** 25 (1969); P. Lyons, J. W. Toevs, and D. G. Sargood, *Nucl. Phys.*, **A130,** 1 (1969); P. Lyons, J. W. Toevs, C. A. Barnes, W. A. Fowler, and D. G. Sargood, *Astrophys. J.*, **159,** 913 (1970).

oo. E. M. Burbidge, G. R. Burbidge, W. A. Fowler, and F. Hoyle, *Rev. Mod. Phys.*, **29,** 547 (1957); P. A. Seeger, W. A. Fowler, and D. D. Clayton, *Astrophys. J. Suppl.*, No. 97, **11,** 121 (1965).

pp. J. D. Larson and R. H. Spear, *Nucl. Phys.*, **56,** 497 (1964).

qq. No really adequate discussion of oxygen burning exists in the literature, but the nature of the problem is very similar to that of carbon burning so the reader may draw his own analogs to reference n. Above $T_9 = 3$ the problem has similarities to silicon burning as described in references q and mm.

rr. W. D. Arnett, *Nature*, **219,** 1344 (1968).

ss. J. R. Patterson, H. Winkler, and C. S. Zaidins, *Astrophys. J.*, **157,** 367 (1969); E. Almqvist, D. A. Bromley, and J. A. Kuehner, *Phys. Rev. Lett.*, **4,** 515 (1960); E. Almqvist, J. A. Kuehner, D. McPherson, and E. W. Vogt, *Phys. Rev.*, **136,** B84 (1964).

tt. It has not been established whether these reactions are ever important. Although they cannot be significant in stars in hydrostatic equilibrium, they may be of significance when the carbon is largely exhausted in a superheated gas following explosive ignition. Despite this uncertainty, experimental information is desirable.

uu. Because of the Coulomb barrier in the final channel this reaction is probably unimportant. There exists the possibility, however, that the Be^8 transfer may occur at larger interaction radii than does the compound nucleus formation between $O^{16} + O^{16}$, in which case this reaction could assume importance.

vv. The special importance of these reactions is described in Section VII of reference q.

lead to excitation energies which differ by as much as 10 keV, corresponding to a factor of 3 uncertainty in the reaction rate.

The list in Table III is presented as a guide to additional specific reactions for which thermonuclear cross sections have a known practical application. The list is long because nature has provided a large number of interesting astrophysical environments. Needless to say, the assemblers of this table are not omniscient, so the table must not be regarded as definitive or complete; future research will undoubtedly point to new problems and applications which are not even envisioned today.

The table lists primarily charged particle reactions of importance in the epochs of thermal fusion in stars. These reactions have the most clearly understood and most urgently needed applications. The list omits most neutron-induced reactions simply because of their large number; important examples of these reactions were presented in Tables I and II covering the area of explosive nuclear synthesis in big and little bangs and the area of heavy element production, respectively. For more complete and detailed listings the reader is referred to Refs. 2, 6, 7, and 11. Charged-particle reactions of interest to explosive nucleosynthesis are not listed for targets with $Z \geqslant 6$. The question of the relative importance of these reactions is not clear, and the potential investigator is referred to Ref. 53. Similarly, only selected reactions of particular importance have been included for the silicon burning epoch, and for a more complete listing and discussion the reader is referred to Ref. 9.

Adjacent to each reaction in the table is the particular known application and the temperature near which the value of $\langle \sigma v \rangle$ is of interest for that application. The references for each reaction cover both the context of its astrophysical interest and the laboratory studies of the reaction which may have been made with the astrophysical problem in mind. The reader should also, of course, consult the standard nuclear data compilations.[54]

The panel suggests that laboratory work could usefully be undertaken on most of the reactions listed in Table III. By simultaneously studying the astrophysical situation, many modestly equipped laboratories could contribute to this exciting field of research.

3. BEAM-FOIL SPECTROSCOPY

Beam-foil spectroscopy[55] applies many of the techniques of nuclear physics to the study of atomic structure in multiply-ionized atoms and to the determination of the mean lives and transition probabilities of their excited electronic levels. A small accelerator is used to generate a beam of ions of the appropriate element, and then the light emitted by these ions (after they have been excited by passing through a thin foil) is analyzed to extract wavelength and lifetime data for the observed transitions. With these techniques many areas of research which are of vital importance in astrophysics, experimental and theoretical atomic physics, plasma physics, etc. have now been opened up to experimenters with only very modest instrumentation budgets; only a few years ago these areas were inaccessible at even very sophisticated laboratories. (An added advantage of this type of research is the fact that the experiments and instrumentation can normally be handled by one person so that a student working in this area can benefit from the traditional, individual training and not get his thesis simply as a cog in a large group.)

This technique can be applied to virtually all elements, limited only by the necessity of being able to generate ions of the element of interest in the ion source of an accelerator. A conventional rf ion source will handle most gaseous elements as well as those which are available in gaseous compounds. For solid materials, the powerful heavy-ion sources[56] developed for mass separators (available commercially as Danfysik Model 910 from Physicon, Boston, Massachusetts) have power requirements of 1.2 to 2.4 kW at present which are a bit too large to make them feasible for terminal installation in most small Van de Graaff accelerators. However, smaller sublimation sources (where the solid material is heated to a temperature at which its vapor pressure is approximately 1 μ and where the vapor is then ionized by electron impact) have been described in the literature for lithium beams,[57] for Al^+, Zn^+, Cu^+, Ag^+, and Fe^+ beams,[58] and for U^+, Sr^+, Ba^+, Te^+, and Be^+ beams.[59]

After analysis by a magnetic or electrostatic analyzer to insure a mono-energetic beam of the proper ion species (the actual choice of beam energy depends very much on the problem under attack, i.e. the ionization state of interest and also the individual transition of interest, since in many cases there is a marked dependence of the relative line intensities on the particle energy[60,61]), the beam is traditionally passed through a thin beryllium or carbon foil (10 to 20 $\mu g/cm^2$). These materials have the advantage of being relatively strong and yet

having a low enough Z to keep the small-angle Rutherford scattering of the beam small. However, one of the interesting fields which should be explored in beam-foil spectroscopy is the effects of other foil materials and of varying foil thicknesses, e.g. the differences between conducting and non-conducting materials, the differences between amorphous and crystalline targets, and the effects of channeling.

Spectroscopic analysis of the light emitted in the radiative decays can be carried out using either narrow-band interference filters or diffraction gratings in conjunction with a spectrometer or a spectrograph. Photographic plates are used as the detectors in a spectrograph, while spectrometers and narrow-band interference filter techniques employ photoelectric detectors. (A description of the specific characteristics and relative merits of some of the particular spectrographs and spectrometers used by the University of Arizona group is presented in the Panel's complete report.[1]) Using photographic plates in a spectrograph, all wavelengths at all positions along the beam path can be recorded simultaneously as shown in Fig. 9.[62] On the other hand, a photoelectric system requires a tedious point-by-point scan of the spectrum and a point-by-point survey of the emitting region along the beam path, and thereby also requires a precise intensity normalization which is not necessary in a photographic system. Unfortunately, the impressive advantages for a spectrograph are offset by the difficulties associated with doing quantitative photometry with photographic plates because of their nonlinearities with respect to photon flux density and with respect to time. There is a great need for a linear detection scheme that will permit the spectrograph to realize its tremendous data-collecting and data-storage potential.

The beam emerging from the 'exciting foil' may contain a wide variety of charge states, and it is important to know which radiative transitions belong to which ionization states of the atom. Such an identification can be accomplished by passing the emerging beam through an external, transverse electric field which will deflect and physically separate particles in the various ionization states.[63] Examining the spectra in these separated beams provides one of the only ways of making unambiguous determinations of the charge states of an atom corresponding to various spectral lines. Some of the other unique characteristics of beam-foil spectroscopy include the possibility of further excitation of an atom from one excited state to an even higher state and the fact that since the decays take place in a good vacuum (rather than in a gaseous discharge) the possibility of collisional de-excitation is minimized so that such states may now decay by radiative transitions.

Because of these unique characteristics, many radiative transitions which could not be observed in conventional spectroscopy can now be studied using beam-foil techniques, including, for example, several of the lines in the nitrogen spectrum[62] in Fig. 9

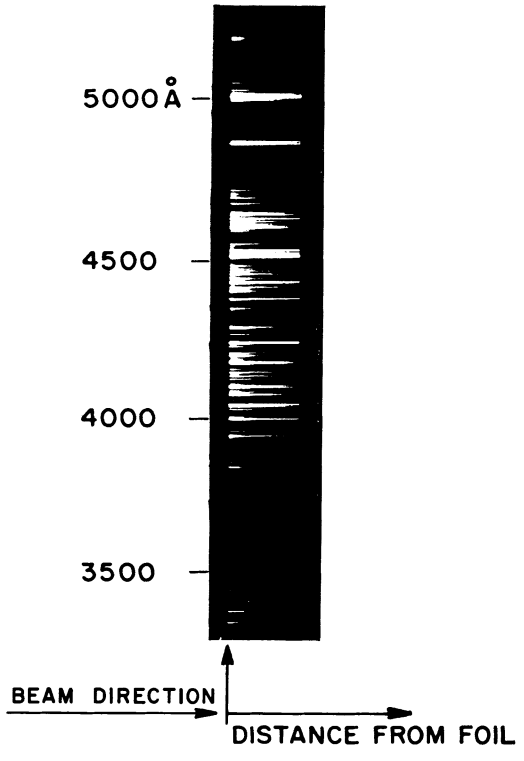

FIG. 9. Visible and near ultraviolet spectrum produced by 0.5 MeV nitrogen ions passing through a carbon foil.[62] The observed transitions take place in the ' beam ' atoms and not in the ' foil ' atoms. In this case the analysis was carried out using a grating spectrograph with a dispersion of 35 Å/mm (in second order).

and 80 of the total of 90 lines seen in a similar experiment using a sodium beam.[64] Because of the high excitations and high ionizations which are available with these techniques and because of the absence of collisional de-excitation, many of these 'new' lines may have important astrophysical applications in understanding the spectra of nebulae, stellar atmospheres, stellar coronae, etc. The

accurate measurement and identification of these previously unknown lines is one of the major areas of research in the field of beam-foil spectroscopy.

The second principal area of research being pursued using beam-foil-spectroscopy techniques involves the measurement of the relative intensity of an emission line as a function of its distance from the foil. When combined with a knowledge of the ion velocity (determined by the magnetic or electrostatic beam analysis with corrections for the energy loss in the foil) this can provide a direct determination of the lifetime of the emitting level. A visual example of this lifetime effect is provided in the decay of the emission lines along the beam axis in Fig. 9 and, more quantitatively, by the plot in Fig. 10 of the relative intensity as a function of

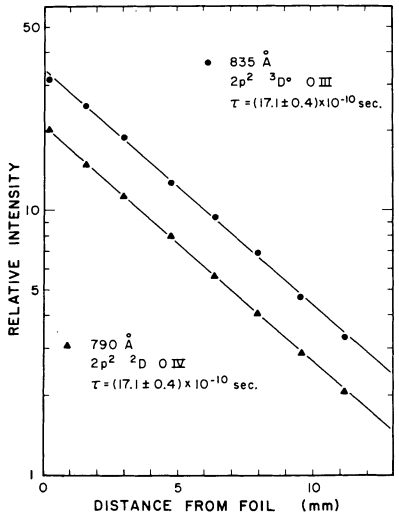

FIG. 10. Plot of relative intensity vs distance from the exciting foil for transitions from the $2p^2\ ^3D^0$ level in O III and the $2p^2\ ^2D$ level in O IV. When combined with a knowledge of the ion velocity these data determine the lifetimes of those levels.

distance from the foil for two oxygen lines in the far ultra-violet.[65] With typical beam velocities of 10^7 to 10^9 cm/sec, this method is applicable to lifetimes in the range 10^{-10} to 10^{-7} sec. Lifetime measurements have been reported using interference filters,[66,67] spectrometers,[60,68] and also spectrographs.[62,64] However, because of the difficulties with photographic plates, in neither of the two spectrograph cases was the quantitative photometry precise enough for a complete analysis as described in the following two paragraphs.

In the simple case where there is no repopulation from higher excited states to the emitting level under study, a plot such as Fig. 10 is sufficient to determine the lifetime of the level. When there is repopulation, however, the effects of the lifetimes (τ_x) of the cascading transitions from the higher levels must be included, and then the population, $N_i(z)$, of the state of interest is given by

$$N_i(z) = N_i(0)\exp(-z/v\tau_i) + \sum_x A_{xi} N_x(0) \cdot \frac{\exp(-z/v\tau_x) - \exp(-z/v\tau_i)}{1/\tau_i - 1/\tau_x},$$

where A_{xi} is the spontaneous emission probability from state-x to state-i. In any measurement (photographic or photoelectric) of the intensity along the beam path (z), the intensity must be integrated over a finite path length (Δz), e.g. Fig. 11, and the intensity in that interval is given by

$$\begin{aligned} I(z,\Delta z) &\propto [N_i(z-\Delta z/2) - N_i(z+\Delta z/2) \\ &\quad + \sum_x A_{xi}\tau_x(N_x(z-\Delta z/2) - N_x(z+\Delta z/2))] \\ &\propto \tau_i N_i(0)\exp(-z/v\tau_i) \\ &\quad \cdot [\exp(\Delta z/2v\tau_i) - \exp(-\Delta z/2v\tau_i)] \\ &\quad + \sum_x \frac{A_{xi} N_x(0)}{1/\tau_i - 1/\tau_x} \{\tau_x \exp(-z/v\tau_x) \\ &\quad \cdot [\exp(\Delta z/2v\tau_x) - \exp(-\Delta z/2v\tau_x)] \\ &\quad - \tau_i \exp(-z/v\tau_i) \\ &\quad \cdot [\exp(\Delta z/zv\tau_i) - \exp(-\Delta z/zv\tau_i)]\}. \end{aligned}$$

The decomposition of the sum of exponentials in $I(z,\Delta z)$ to yield τ_i, and in addition values for as many of the τ_x, $N_i(0)$, and $N_x(0)$ as possible, is the basic problem in the analysis of beam-foil lifetime

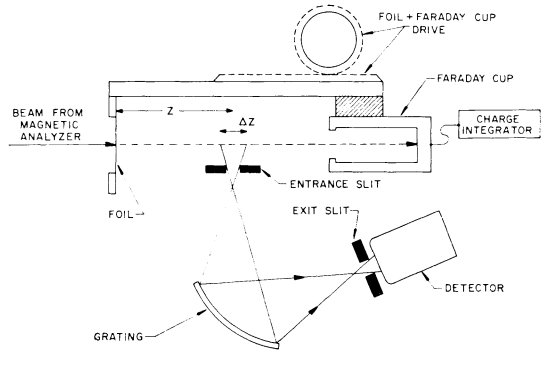

FIG. 11. Typical experimental geometry for lifetime measurements with a spectrometer. Since no lenses or windows are used, this geometry can be used for measurements in the vacuum ultraviolet. In the figure, the jaws of both slits are normal to the plane of the paper.

measurements. Several authors have developed computer programs for this calculation, and at least two programs have been made available for use by others.[69,70] Although machine computation has been widely used, simple graphic methods are often adequate. Heroux[68] described fully an example of graphical analysis of a N IV decay curve, from which he extracts two exponential terms plus a constant background. His analysis also illustrates the advantages of measuring several decay curves for other transitions from upper states which can cascade into lower states of interest; a system of interrelated transitions can often be unraveled when a single transition cannot. Every author who has attempted this analysis stresses the necessity for accuracy in the decay-curve measurements if the sum is to be decomposed at all. It is this necessity for precision that would seem to favor a counting experiment, with good statistics, over a photographic measurement of the decay curve.

The following precautions must be taken in obtaining accurate relative intensities for lifetime determinations using point-by-point photoelectric techniques (e.g. Fig. 11). Since the beam undergoes small-angle scattering in the foil and diverges as it moves downstream, the light source expands and becomes less dense downstream from the foil. Therefore, it is essential that the slit and the aperture of the spectrometer accept photons from all parts of this enlarged source. Otherwise, one would observe a decrease in the photon flux downstream from the foil that reflects acceptance geometry instead of the lifetime of the decay. Furthermore, for point-by-point measurements some means must be provided to take account of fluctuations of the beam current which could introduce variations in intensity that have nothing to do with atomic lifetimes. This normalization is usually provided by a detector at a fixed location (fixed *with respect to the foil*), preferably near the foil where the beam is brightest; the moveable detector (moveable *with respect to the foil*) then counts for that period during which the fixed detector is accumulating a preset number of photons. Ideally the fixed detector would be sensitive only to the particular wavelength counted in the moveable detector, but in most measurements reported so far the monitor has been an unfiltered photomultiplier. Alternatively, the beam current can be integrated in a Faraday cup downstream from the foil. This latter method assumes that the charge-state distribution, the population of excited states, and the beam integration remain constant in spite of the changes which can take place in the foil during bombardment. The reliable integration of heavy-ion beams also introduces additional problems associated with the suppression of secondary electrons[37] so that it would be wise to keep a constant separation between the foil and the Faraday cup during any set of runs. Although it is less direct and less ideal than monitoring the light emission of the particular wavelength of interest with a fixed detector, beam-current integration has, however, been used successfully in several experiments, e.g. Refs. 66 and 71.

The interest in atomic lifetimes stems from their use in analyzing the composition of stars, the interstellar medium, and terrestrial plasmas. The measurements that one would list as most needed depend upon the particular application and interest. Garstang[72] has discussed astrophysical needs that can be attacked by the beam-foil method. To quote from his paper:

'Ions which are worthy of study include almost all stages of ionization of C, N, O, Ne, Na, Mg, Si, S, Ca, Fe, Ni. . . . If asked to pick out one group that would be more useful than any other, I think I would say that one should select all stages of ionization of iron, and try to determine the transition probabilities of the lines connecting the ground configuration with the first three or four excited configurations, and the transition probabilities for the lines connecting these excited configurations. I think I would give second priority to various lines of silicon, and after that to the stronger lines of carbon, nitrogen, and oxygen. . . . Further work is badly needed on the transition probabilities of lines involving highly excited states of important elements, particularly Fe I and other transition group elements. . . . Another area of importance for traditional spectroscopy is in the lines of the rare earths. . . .'

Garstand also lists specific transitions that are important in judging the validity of various approximations used in theoretical calculations. He also notes the increasing interest in the far ultraviolet spectrum.

Bahcall[73] has compiled a list of 114 lines of particular importance in the interpretation of quasar absorption spectra for which reliable transition probabilities are needed. Of the 114 lines, 101 are in the UV wavelength range between 900 and 1900 Å.

Aller[74] tabulates and assesses the reliability of *f*-values used in the determination of the abundance of all elements observed in the sun: nearly half of these *f*-values he judges 'doubtful' or 'poor', nearly

two thirds of them are estimated theoretically, since experimental measurements are not available. Aller's book includes a complete discussion of abundance measurements in stars and nebulae and a good review of the availability of the atomic transition probabilities needed for this analysis.

Glennon and Wiese[75] have compiled a bibliography of the literature on transition probabilities, both theory and experiment, that is indispensable to those interested in this field. In addition to the primary literature on particular values, they list review articles, critical summaries, and compilations. They summarize the over-all availability of atomic transition probabilities as follows:

'From the compilation it may be seen that for a few of the 92 natural elements no material is available. For many other elements data exist only for the neutral atom and the first stage of ionization. Furthermore, the number of transitions treated is often quite small, and sometimes only the transition probability for the resonance line or for forbidden transitions are available.'

Wiese and his co-workers at the National Bureau of Standards are making a critical compilation of all measured and calculated values of atomic transition probabilities. Their review of the region $Z = 1$–10 has been published,[76] and work on higher values of Z is in progress. Their critical comparison of different values makes use of the fact that transition probabilities between corresponding levels in an isoelectronic sequence follow a smooth functional dependence on $Z, f(Z)$, just as the term values do. They are thus able to compare measured or calculated lifetimes for a particular transition in one ion with the corresponding lifetime in other ions. On the basis of their survey of the first ten elements, they find that measurements of transitions between low-lying levels would be useful from the point of view of establishing the shape of the function $f(Z)$ for complex configurations. The following transitions are especially important, since theoretical treatments have not as yet been successful for these cases because of strong configuration interaction:

$2s^2 2p\ ^2P - 2s^2 3s\ ^2S$ transition in B I (2497 Å), C II (858 Å), N III (452 Å), O IV (279 Å), and Ne V (174 Å)

$2s^2 3s\ ^2S - 2s^2 3p\ ^2P$ transition in B I (11161 Å), C II (6579 Å), N III (4099 Å), O IV (3066 Å)

$2s^2 2p\ ^2P - 2s 2p^2\ ^2P$ transition in B I (1378 Å), C II (904 Å), N III (685 Å), O IV (554 Å)

$2s^2 2p\ ^2P - 2s 2p^2\ ^2S$ transition in B I (1537 Å), C II (1036 Å), N III (764 Å), O IV (609 Å)

$2s^2 2p^2\ ^3P - 2s 2p^3\ ^3P$ transition in C I (1329 Å), N II (916 Å), and O III (703 Å).

It should be noted that most of these wavelengths lie in the far ultraviolet. Note also that nearly all the beams needed for these measurements can be produced with an rf ion source. As Wiese extends his analysis to higher values of Z, he will certainly be able to point out further measurements that are critical in guiding and assisting the theoretical calculation and resolving discrepancies.

4. SOLID-STATE PHYSICS

The interaction between nuclear physics and solid-state physics has been a two-way street with the discoveries and products of one field often being utilized as research tools by the other. In the present case we are concerned with the application of nuclear physics as a research tool in solid-state physics. The specific areas of interest discussed below include the use of accelerator beams for (1) the analysis of elemental and/or isotopic compositions, (2) studies of the properties of materials by ion implantation, and (3) studies of the structure of solids and the passage of charged particles through matter. All of these areas represent rewarding opportunities for investigators with interest and insight into the physics of the solid state and with access to the tools of nuclear physics. (As in the areas of nuclear astrophysics and beam-foil spectroscopy discussed above, the experimentation in solid-state physics will require ion sources and techniques for producing a wide variety of beams and will require some form of magnetic beam analysis for selecting the species of interest.)

In the area of materials analysis,[77] nondestructive testing can be carried out by using activation techniques (bombarding the sample with thermal neutrons, fast neutrons, electrons, bremsstrahlung, or charged particles and then measuring specific, residual radioactivities) or by analysis of the prompt radiations produced during the actual bombardment. Of these two, the analysis of prompt radiations is much less highly developed and, therefore, a more promising area for research with small accelerators. Even in activation analysis, however, much basic data are still needed, and new applications to problems in other fields may confidently be expected.

For activation analysis the most common technique is to place the sample in the thermal neutron flux in a nuclear reactor. However, residual activities can also be produced using fast neutrons, bremsstrahlung, or charged particle beams. For fast neutron activation, a good compact discussion of accelerator neutron sources including their operating characteristics, costs, and detection sensitivities is given by Strain.[78] For the elements N, O, F, Al, Si, P, Cr, Mn, Cu, Y, Mo, and Nb the lower limits of detection sensitivity (for a 10 minute irradiation at 10^8 neutrons/cm^2/sec) fall in the range from 40 to 400 μg. A useful compilation of sensitivities in fast neutron activation has been prepared by Cuypers and Cuypers.[79] For charged-particle activation, Coulomb barrier effects restrict low-energy accelerators to studies of light elements, using primarily beams of protons, deuterons, and He^3.[80] An excellent discussion and list of references for charged-particle activation analysis is given by Tilbury.[77] Another important limitation on charged-particle activation arises from the short range of penetration of the charge particles in matter, e.g. only 50 μm of silicon for a 2 MeV proton. While this short penetration prevents bulk analysis of materials, it can also be an important advantage for the analysis of surface effects. For example, the amount of carbon in silicon has been measured at the 5–10 ppm level using 3.0-MeV deuterons and the $C^{12}(d,n)N^{13}$ reaction. By etching successive surface layers away between irradiations it was found that sawing and lapping operations introduced carbon into the samples down to depths of between 100 and 200 μm.[81]

The observation of the prompt radiations produced by bombardment with neutrons, γ-rays, or charged-particle beams can also be used for material analyses. The $S^{32}(d,p)S^{33}$ reaction has been used to measure the amount of sulfur in a thin film on a copper-nickel alloy. A sulfur surface density of 10^{-7} g/cm^2 was easily measured. Since the area bombarded was 0.5 mm^2, the actual weight of sulfur needed for the test was 2×10^{-10} g.[82] In addition, with prompt analysis advantage can be taken of the fact that some nuclear reactions possess sharp energy resonances. The 1373-keV resonance in the $F^{19}(p,\alpha\gamma)O^{16}$ reaction can be used for an analysis of fluorine with a sensitivity of 10 parts per billion.[83]

Although the area of materials analysis is one of the oldest applications of nuclear reactions to the study of solids, research is still needed for the introduction and development of clever ideas and new approaches by which more sensitivity or more specificity can be obtained. In particular, the use of charged nuclear-particle beams for analyzing materials and for studying physical processes which occur at surfaces requires much more thorough investigation. The richness of the techniques, perhaps especially where prompt analysis of radiation is used, is such that collaboration between small accelerator groups and groups in other research fields should be most rewarding.

Ion implantation (the introduction of atoms into solids by bombardment at keV to MeV energies) has broad applicability to solid-state physics and to the fields of nuclear and atomic physics as well. For example, nuclear magnetic moments may be determined from studies of hyperfine interactions of atoms implanted into ferromagnetic materials, and then these known nuclear magnetic moments may be used via the same interactions to investigate electromagnetic fields in solids. Another aspect of ion implantation concerns the fact that during implantation the ion slows down by losing energy through electronic and nuclear collisions.[84–86] In the nuclear collisions a large amount of energy is transferred, and in a crystal this will result in the production of a disordered region along the ion's path where the atoms have been displaced from their lattice sites. At low doses, the disordered regions around individual tracks are spatially separated; at high doses, they overlap, and the disorder saturates. These radiation damage effects can, however, be removed, and the lattice order restored by annealing the material at temperatures of a few hundred degrees centigrade. In fact, by the use of heated substrates ($T>200$ °C for Ge and $T>300$ °C for Si), implantations can be performed to doses of 10^{14} to 10^{15} ions/cm^2 without large amounts of lattice disorder. Even though this damage can be removed so that ion implantation can be used as a technique for other investigations without destroying the crystalline structure of the material in the process, there is still a need for further study of the lattice disorder effects themselves, and the variation of the fraction of implanted ions at substitutional sites in a lattice as a function of implantation temperature and implantation dose.

One of the areas in which ion implantation can be used as a technique is the field of doping semiconductor devices. In this way doping concentrations[87,83] and distributions can be obtained which are not achievable by conventional, thermal diffusion techniques. An example of this is the produc-

tion of a two-detector ($dE/dx, E$) telescope in a single piece of silicon by using 22-MeV boron ions as dopants to generate $2\,p$–n junctions in the one piece of silicon.[89] By similar techniques thin magnetic films or thin superconducting layers can be produced in solid substrates.

Another area open for active collaboration between solid-state and nuclear physicists is the study of the solid-state environment made by using the nuclear magnetic dipole, electric monopole and electric quadrupole moments as probes. Electron spin resonance, nuclear magnetic resonance, perturbed angular correlation and Mössbauer experiments are all examples of the types of measurements used in this area. Most of these studies have been carried out using stable or radioactive isotopes which are introduced into the solid during crystal growth or by thermal diffusion. However, in the case of Mössbauer measurements and perturbed angular correlations it is also possible to introduce the atoms dynamically by ion implantation. Excited nuclear states are populated via nuclear reactions using the accelerator beam, and then the kinematics of the nuclear reaction will cause these excited nuclei to recoil into a solid-state environment where their decay is observed. For Mössbauer studies[90] this has the advantage of making available a much wider variety of decaying states than can be obtained using radiochemistry techniques.

In perturbed-angular-correlation experiments[91] the initial nuclear reaction is also used to populate or select residual nuclei with definite spin orientation, e.g. the Litherland–Ferguson method[92] which limits the magnetic substate population of Y in the nuclear reaction $X(a,b)Y$ by detecting the outgoing particles, b, at either 0° or 180° relative to the incident beam. After implantation of this aligned nucleus, during the lifetime of the excited state interactions between the nuclear moments and the electromagnetic fields in the solid may alter the initial alignment and, thus, perturb the angular correlation from what it would have been in a field-free environment. An analysis of the resulting perturbation can be used in two ways. With the aid of known external fields and an understanding of the extranuclear fields in solids perturbed-angular-correlation measurements can be used to determine the magnetic and/or electric moments for excited nuclear states. On the other hand if the nuclear moments and the mean life of the state are known, perturbed angular correlations become a tool for studying the extranuclear electromagnetic fields for various atomic or solid-state environments.

In making perturbed-angular-correlation measurements it is necessary that the nuclear state be populated with significant spin orientation and that the kinematics of the nuclear reaction, the lifetime of the state, and the stopping power of the target be consistent with implanting the residual nucleus in the desired solid state environment. There are two methods for observing perturbed angular correlations: time differential and time integral. The time differential technique requires the measurement of the γ-ray yield at a given angle as a function of the time since formation of the state (detection of particle b). It is essentially a time measurement and requires that the time resolution of the experimental apparatus is small compared to the perturbation times and to the mean life of the nuclear state; the γ-ray detectors must be located at distances so that the angular resolution and the time resolution are adequate to resolve the time-dependent anisotropies of the perturbed correlation. With the present experimental limitations of 200 to 300 psec on nuclear time difference measurements,[93] the time-differential method is applicable only for states with lifetimes greater than about 1 nsec, (e.g. the study[94] of the 1.131-MeV level in F^{18} which has a mean life of 225 nsec, see Fig. 12). The time integral method[95] measures the γ-ray yield from the aligned state as a function of angle and is essentially the time integral of the angular correlation over the nuclear lifetime. The time-integral technique is not as accurate as the time-differential technique, but has the advantage that it can be used for much shorter lifetimes than the time-differential method. (It should be cautioned that both types of perturbed angular correlation measurements require fairly sophisticated experimental techniques and a rather large amount of very fast and complex electronic gear.)

There are a large number of solid-state problems for which perturbed angular correlation measurements can provide important data by acting as a microscopic probe of the electromagnetic fields in solids. Experiments have been performed to measure electric field gradients in single crystals and poly crystals,[91] and the perturbed angular correlation technique can also be used to study time-dependent quadrupole interactions. These methods have most often been applied to the study of magnetic fields in solids. Hyperfine fields in ferromagnetic materials have been investigated using time-integral techniques[95] with Coulomb excitation and using time-differential techniques[96,97]

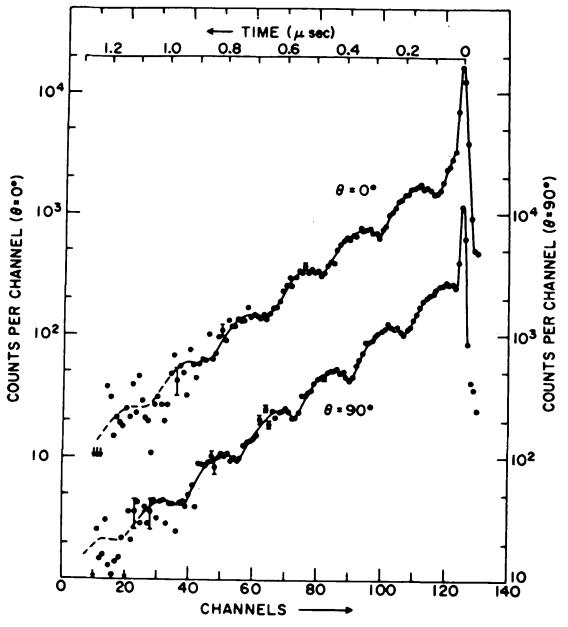

FIG. 12. Data from a time-differential measurement of a perturbed angular correlation produced by a static magnetic field. In this case,[94] the 1.131-MeV level in F^{18} (τ = 225 nsec) was aligned by the $O^{16}(He^3, p)F^{18}$ reaction in the 180° geometry of Litherland and Ferguson.[92] The modulations on the decay curves correspond to a Larmor precession of the γ-ray correlation.

with the $F^{19}(p,p')$ reaction populating the 198-keV first excited state which has a lifetime of 125 nsec. Perturbed angular correlations can also be applied to the study of magnetic fields in superconductors,[98,99] the study of hyperfine fields of free atoms (by recoiling the aligned residual nuclei into vacuum or into a gas[100] where time-integral measurements can be made as function of pressure, i.e. the time between collisions), and the study of range and range straggling for heavy ions.[101] In the latter case, a known thickness of the stopping material in question is sandwiched between a thin target and a ferromagnetic backing; the angular correlations of the fraction of recoil nuclei that reach the ferromagnetic backing will be strongly perturbed while the correlations of the nuclei that do not reach the backing will be unaffected.

In studies of the interactions of charged particles with matter, the measurement of ranges and energy-loss data not only provides necessary information for ion implantation studies but also provides a means for studying atomic collisions and the nuclear and electronic processes by which ions lose energy in solids.[84,85] One aspect of the passage of charged particles through matter which has stimulated considerable interest recently is the phenomenon of channeling in single crystals.

Whenever a beam of accelerated atomic particles enters a crystal within a certain critical angle ($\psi_{\frac{1}{2}}$) of a major axis (or plane), it then becomes 'channeled'; i.e. each time it approaches one of the aligned rows of lattice atoms, the gradually increasing Coulomb repulsion between the projectile and the lattice atoms is sufficient to steer it away again,[102] thereby preventing violent nuclear collisions from occurring. (A forbidden region (~0.1 Å in radius) is generated around the atomic rows.) In making channeling measurements, orientations and alignments with accuracies of 0.2° are desirable, and can usually be obtained in situ by observing the channeling behavior of protons in the crystal.[103] Because of the dechanneling effects of surface films such as oxide layers or carbon build-up, careful cleaning of the crystal surface and good vacuum conditions in the target chamber are necessary.

One obvious consequence is that the rate of energy loss is much smaller for a channeled particle, and hence it can penetrate more deeply than in an amorphous target. Nuclear stopping depends much more strongly on the impact parameter than does electronic stopping, and therefore channeling can be utilized to suppress nuclear stopping almost entirely, thereby enabling electronic stopping to be investigated over a much wider energy range than would otherwise be possible. Figure 13 illustrates the effects of shielding and open channels in a crystal lattice,[104] while Fig. 14 demonstrates the effect of channeling on the energy lost by charged particles passing through a silicon single crystal.[105] The most sensitive ways of investigating the mechanism of channeling are provided by those interactions which require the smallest impact parameters, e.g. inner-shell X-ray production,[106] Rutherford scattering,[107] and nuclear reactions.[103] The yield for such interactions can fall to essentially zero for channeled particles as shown in Fig. 15. The non-zero yield at 0° is a measure of the unchanneled fraction of the beam; a study of this fraction can determine how much dechanneling takes place at the crystal surface, and in some cases (by an energy analysis of the backscattered particles) this method can also be used to study dechanneling as a function of penetration depth into the crystal.

Although many aspects of channeling still require further study, the understanding of the steering process involved is now sufficiently well

established so that the channeling effect can be used as a tool for studying certain properties of crystals. Channeling can be used to orient a crystal with an accuracy as good as $\pm 0.02°$; an accuracy of $\pm 0.1°$ can be achieved in about 10 to 15 minutes. Radiation damage and lattice disorder in a crystal can be studied with channeling by making use of the fact that atoms displaced more than ~ 0.1 Å will be able to interact with the channeled beam and contribute to any nonzero yield at 0° in Fig. 15. By an energy analysis of the backscattered particles in this case, lattice disorder can be measured as a function of the depth in the crystal.

Channeling measurements can also be used to determine the location of foreign atoms in crystals.[87,108] If the foreign atom is on a lattice

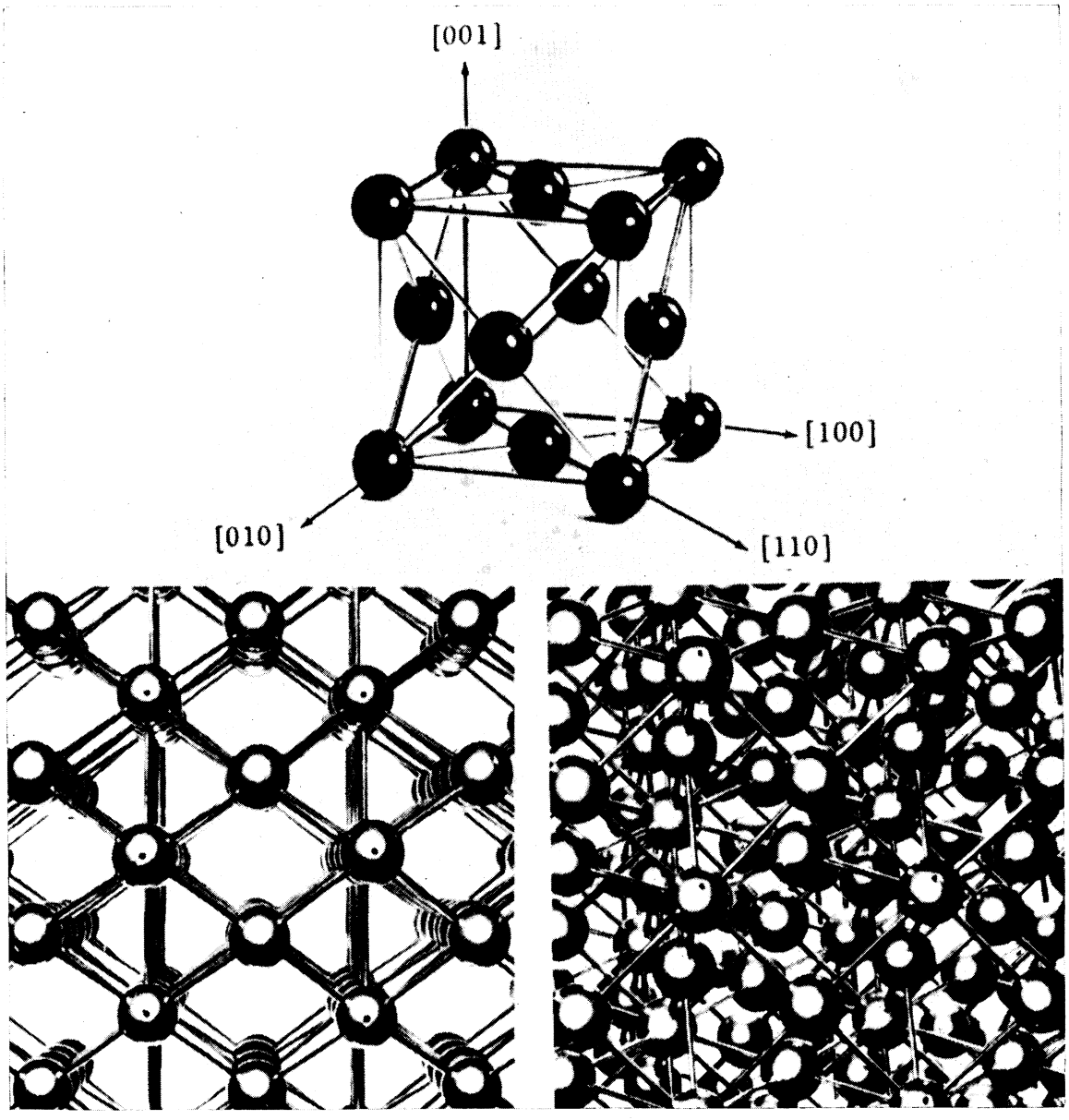

FIG. 13. A face-centered cubic crystal lattice viewed from different directions to illustrate the 'open' nature of the channels.

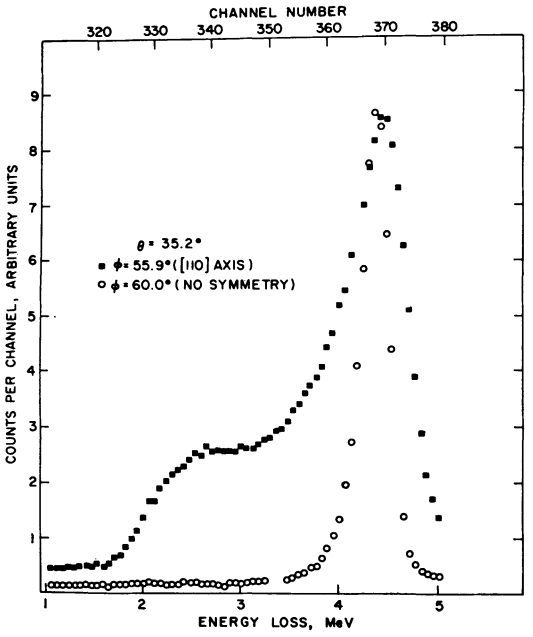

FIG. 14. Energy loss spectra for 40-MeV α-particles passing through a 0.1-mm thick silicon single crystal. The two spectra (plotted to equal height) refer to the [110] direction and to a direction of no symmetry.

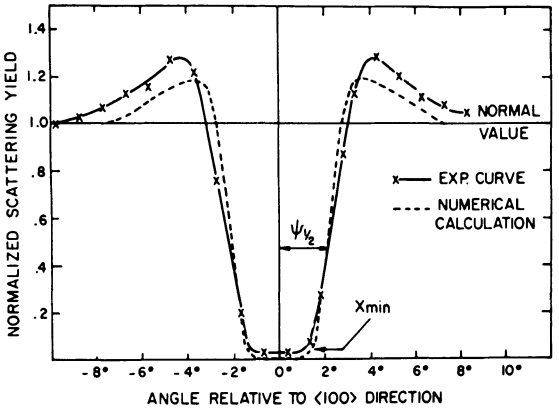

FIG. 15. The experimental and calculated axial 'dip' in Rutherford scattering yield for 480-keV protons incident along a ⟨100⟩ direction in tungsten at 390 °K.

site (i.e. substitutional), it will be unable to interact with the channeled beam, and hence a large attenuation in its interaction yield will occur. If, on the other hand, the foreign atom is interstitial, then along some of the major directions it will not lie within the forbidden region (~0.1 Å radius) around the atomic rows; consequently the channeled beam can interact normally with it, and no attenuation in yield will be observed. Hence, by investigating simultaneously the interaction of the beam with both the lattice and the foreign atoms, one obtains a quantitative measure of the distribution of foreign atoms between substitutional and specific interstitial positions.

Of course, to apply the method, it must be feasible to detect the interaction of the beam with a small concentration of foreign atoms in the presence of the far more numerous atoms of the lattice. Whenever the foreign atom is heavier than the lattice atom, Rutherford scattering can be used to distinguish between them.[87] If the foreign atom has an atomic number less than ~10, it can usually be detected by means of a specific nuclear reaction, such as (p,α), (p,γ), or (d,p), while Rutherford scattering can still be used to study the interaction with the lattice.[109] One of the most striking aspects of ion implantation is that the lattice location of the implanted atoms depends on the chemical nature of these atoms, their position in the periodic table, and Fig. 16 illustrates the use of channeling (using Rutherford scattering as the probe) to determine the location of three different implanted heavy ions in silicon crystals.[88] These examples demonstrate how channeling studies along two or more axes can be used to determine by triangulation the exact location of the foreign atoms in a crystal. In the Au case, the interaction yield shows no orientation dependence in that the peaks observed when the beam is channeled along the ⟨111⟩ or ⟨110⟩ axes are indistinguishable from

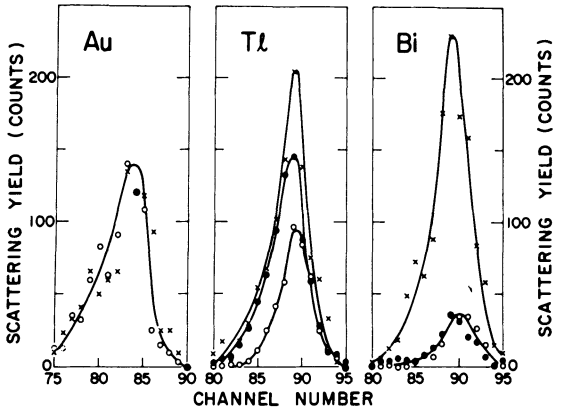

FIG. 16. Orientation dependence of the backscattered yield from heavy foreign ions implanted into silicon.[88] Spectra were obtained with a He^+ beam incident along: O, a ⟨111⟩ axis; ●, a ⟨110⟩ axis; X, a random direction.

that for the random (i.e. *un*-channeled) beam. Hence the Au atoms must be in some sort of random positions located well away from the atomic rows.

The interaction with Bi, on the other hand, falls almost to zero along both the ⟨111⟩ and ⟨110⟩ axes, indicating that ~90% of the Bi atoms lie at the intersection of these two atomic rows. The Bi atoms must therefore be on substitutional sites.

The third case, Tl, is a particularly intriguing one in that the interaction is reduced by about twice as much for the beam incident in the ⟨111⟩ direction as in the ⟨110⟩ direction. This indicates that there are about twice as many Tl atoms located along the ⟨111⟩ rows as along the ⟨110⟩ rows. From this it can be concluded that, although some of the Tl atoms are on lattice sites, an approximately equal number are located in the regular interstitial holes along the ⟨111⟩ direction.

Channeling would seem to be a particularly exciting and suitable area for research in solid-state physics with a small accelerator, both in the study of the phenomenon itself and in the utilization of the phenomenon for studying the properties of crystals and for investigating many problems relating to ion implantation.

As a conclusion to their presentation, this 'ad hoc panel' finds that there is still a large body of very interesting and very valuable research to be carried out using low-energy accelerators on modest budgets, and the panel hopes that workers in these situations will find some areas of interest in the many, diverse fields covered in this report.

REFERENCES

1. *New Uses for Low-Energy Accelerators;* Ad Hoc Panel on New Uses for Low-Energy Accelerators of the Committee on Nuclear Science, National Research Council; National Academy of Science; 1968. (A limited number of copies of their complete report are available from the Physics Section of the National Science Foundation.)
2. E. M. Burbidge, G. R. Burbidge, W. A. Fowler, and F. Hoyle, *Rev. Mod. Phys.*, **29,** 547 (1957).
3. P. D. Parker, J. N. Bahcall, and W. A. Fowler, *Astrophys. J.*, **139,** 602 (1964).
4. W. A. Fowler, G. R. Caughlan, and B. A. Zimmerman, *Ann. Rev. Astron. Astrophys.*, **5,** 525 (1967).
5. W. A. Fowler and W. E. Stephens, *Am. J. Phys.*, **36,** 289 (1968).
6. D. D. Clayton, *Principles of Stellar Evolution and Nucleosynthesis* (McGraw-Hill Book Co., Inc., New York, 1968).
7. R. L. Macklin and J. H. Gibbons, *Rev. Mod. Phys.*, **37,** 166 (1965).
8. R. V. Wagoner, *Astrophys. J. Suppl.*, No. 162 (1969).
9. D. Bodansky, D. D. Clayton, and W. A. Fowler, *Astrophys. J. Suppl.*, No. 148 (1968).
10. D. D. Clayton, *Astrophys. J.*, **139,** 637 (1964).
11. P. A. Seeger, W. A. Fowler, and D. D. Clayton, *Astrophys. J. Suppl.*, No. 97 (1965).
12. R. L. Macklin and J. H. Gibbons, *Phys. Rev.*, **159,** 1007 (1967).
13. M. C. Moxon and E. R. Rae, *Nucl. Instr. Methods*, **24,** 445 (1963); R. L. Macklin, J. H. Gibbons, and T. Inada, *Nucl. Phys.*, **43,** 353 (1963).
14. P. D. Parker and R. W. Kavanagh. *Phys. Rev.*, **131,** 2578 (1963).
15. K. Nagatani, M. R. Dwarakanath, and D. Ashery, *Nucl. Phys.*, **A128,** 325 (1969).
16. D. F. Hebbard and J. L. Vogl, *Nucl. Phys.*, **21,** 652 (1960).
17. e.g. T. A. Tombrello and P. D. Parker, *Phys. Rev.*, **131,** 2582 (1963); T. A. Tombrello, *Nucl. Phys.*, **71,** 459 (1965).
18. W. Neng-ming, V. N. Novatskii, G. M. Asetinskii, and C. Nai-kung, *J. Nucl. Phys. (USSR)*, **3,** 1064 (1966).
19. A. D. Bacher and T. A. Tombrello (to be published).
20. M. R. Dwarakanath and H. C. Winkler, *Bull. Am. Phys. Soc.*, **12,** 1140 (1967); *Bull. Am. Phys. Soc.*, **12,** 16 (1967); private communication.
21. R. M. May and D. D. Clayton, *Astrophys. J.*, **153,** 855 (1968).
22. E. K. Warburton, J. W. Olness, and D. E. Alburger, *Phys. Rev.*, **140,** B1202 (1965).
23. J. B. Marion, C. A. Ludemann, and P. G. Roos, *Bull. Am. Phys. Soc.*, **11,** 332 (1966).
24. D. C. Hensley, *Nucl. Phys.*, **85,** 461 (1966); *Astrophys. J.*, **147,** 818 (1967).
25. D. E. Alburger and E. K. Warburton, *Phys. Rev.*, **152,** 914 (1966).
26. P. A. Seeger and R. W. Kavanagh, *Nucl. Phys.*, **46,** 577 (1963).
27. D. D. Clayton, *Phys. Rev.*, 128, 2254 (1962).
28. H. M. Loebenstein, D. W. Mingay, H. Winkler, and C. S. Zaidins, *Nucl. Phys.*, **A91,** 481 (1967).
29. P. D. Parker, *Phys. Rev.*, **173,** 1021 (1968).
30. W. Whaling, *Handbuch der Physik*, **34,** 193 (1958); D. Demirlioghu and W. Whaling, Calif. Instit. of Tech. Report (1962) (unpublished).
31. C. F. Williamson, J. P. Boujot, and J. Picard, CEA-R 3042 (Centre d'Etudes Nucléaires de Saclay, 1966).
32. L. C. Northcliffe, *Phys. Rev.*, **120,** 1744 (1960); *Ann. Rev. Nucl. Sci.*, **13,** 67 (1963); L. C. Northcliffe and R. F. Schilling, *Nuclear Data Tables*, **A7,** 233 (1970).
33. G. B. Bishop, *Nucl. Instr. Methods*, **62,** 247 (1968).
34. R. G. Miller and R. W. Kavanagh, *Nucl. Instr. Methods*, **48,** 13 (1967).
35. C. Chasman, K. W. Jones, R. A. Ristinen, and D. E. Alburger, *Phys. Rev.*, **159,** 830 (1967).
36. S. L. Blatt, D. B. Nichols, R. G. Arns, J. D. Goss, and H. J. Hausman, *Nucl. Instr. Methods*, **61,** 232 (1968).
37. H. M. Loebenstein, D. W. Mingay, and C. S. Zaidins, *Nucl. Instr. Methods*, **33,** 175 (1965).
38. C. S. Zaidins, Calif. Inst. of Tech. Report (1962) (unpublished).
39. H. A. Enge, M. A. Wahlig, and I. Aanderaa, *Rev. Sci.*

Instr., **28,** 145 (1957); P. D. Barnes, D. Biegelson, J. R. Comfort, and R. O. Stephen, WNSL Internal Report #25, Yale University (1965) (unpublished).
40. A. B. Brown, C. W. Snyder, W. A. Fowler, and C. C. Lauritsen, *Phys. Rev.*, **82,** 159 (1951).
41. L. P. Robertson, B. L. White, and K. L. Erdman, *Rev. Sci. Instr.*, **32,** 1405 (1961).
42. G. W. Grodstein, NBS Circular #583 (1957).
43. E. F. Plechaty and J. R. Terrall, UCRL-50178 (1966).
44. e.g., R. L. Heath, AEC Rep. IDO-16880 (1964); Ref. 14.
45. L. Salmon, *Nucl. Instr. Methods*, **14,** 193 (1961).
46. e.g., S. J. Mills, *Nucl. Instr. Methods*, **81,** 217 (1970); R. G. Heimer, R. L. Heath, M. Putnam, and D. H. Gipson, *Nucl. Instr. Methods*, **57,** 46 (1967); M. A. Mariscotti, *Nucl. Instr. Methods*, **50,** 309 (1967).
47. R. W. Kavanagh, *Nucl. Phys.*, **15,** 411 (1960).
48. P. D. Parker, *Phys. Rev.*, **150,** 851 (1966).
49. P. Lyons, J. W. Toevs, and D. G. Sargood, *Nucl. Phys.*, **A130,** 1 (1969).
50. R. E. Brown, *Phys. Rev.*, **125,** 347 (1962).
51. J. B. Marion and W. A. Fowler, *Astrophys. J.*, **125,** 221 (1957).
52. S. Hinds, H. Marchant, and R. Middleton, *Nucl. Phys.*, **51,** 427 (1964).
53. R. V. Wagoner, *Astrophys. J. Suppl.*, No. 162 (1969).
54. F. Ajzenberg-Selove and T. Lauritsen, 'Energy-Levels of Light Nuclei VII' (to be published); *Nucl. Phys.*, **11,** 1 (1959), **78,** 1 (1966), **A114,** 1 (1968). For data on more massive nuclei the reader should consult P. M. Endt and C. Van der Leun, *Nucl. Phys.*, **34,** 1 (1962), **A105,** 1 (1967); C. M. Lederer, J. M. Hollander, and I. Perlman, *Table of Isotopes*, 6th ed. (John Wiley and Sons, Inc., New York, 1967); *Nuclear Data Sheets 1959–1965* (Academic Press, New York, 1966); *Landolt-Börnstein Energy Levels of Nuclei: A = 5 to A = 257*, K. Hellwege, ed. (Springer-Verlag, Berlin, 1961).
55. e.g. *Proceedings of the Conference on Beam-Foil Spectroscopy, University of Arizona, 1967* (Gordon and Breach, New York, 1968).
56. K. O. Nielsen, *Nucl. Instr. Methods*, **1,** 289 (1957).
57. R. R. Carlson, p. 475 in *Nuclear Research with Low Energy Accelerators* (Academic Press Inc., New York, 1967).
58. G. P. Magnuson, C. E. Carlston, P. Mahadevan, and A. R. Comeaux, *Rev. Sci. Instr.*, **36,** 136 (1965).
59. Layton, Stebbings, Brackman, Fite, Ott, Carlston, Comeaux, Magnuson, Mahadevan (unpublished). May be obtained by writing to W. L. Fite, Physics Department, University of Pittsburgh.
60. S. Bashkin, D. Fink, P. R. Malmberg, A. B. Meinel, and S. G. Tilford, *J. Opt. Soc. Amer.*, **56,** 1064 (1966).
61. W. Whaling, R. B. King, and P. L. Smith, Paper No. 24 in Ref. 55.
62. U. Fink, G. N. McIntire, and S. Bashkin, *J. Opt. Soc. Amer.*, **58,** 475 (1968).
63. P. R. Malmberg, S. Bashkin, and S. G. Tilford, *Phys. Rev. Letters*, **15,** 98 (1965).
64. L. Brown, W. K. Ford, Jr., V. Rubin, W. Trächslin, and W. Brandt, Paper No. 2 in Ref. 55.
65. W. S. Bickel, *Phys. Rev.*, **162,** 7 (1967).
66. J. A. Jordan, Jr., G. S. Bakken, and R. E. Yager, *J. Opt. Soc. Amer.*, **57,** 530 (1967).
67. A. S. Goodman and D. J. Donahue, *Phys. Rev.*, **141,** 1 (1966).
68. L. Heroux, *Phys. Rev.*, **153,** 156 (1967).
69. F. Grard, University of California Radiation Laboratory Report UCRL 10153, TID-4500, 17th ed. (unpublished).
70. P. R. Rogers, M.I.T. Laboratory for Nuclear Science Technical Report No. 76 (1962) (unpublished).
71. K. Berkner, W. S. Cooper III, S. N. Kaplan, and R. V. Pyle, *Phys. Letters*, **16,** 35 (1966).
72. R. H. Garstang, Paper 19 in Ref. 55.
73. J. N. Bahcall, *Astrophys. J.*, **153,** 679 (1968).
74. L. H. Aller, *The Abundance of the Elements* (Interscience Publishers, Inc., New York, 1961).
75. B. M. Glennon and W. L. Wiese, N.B.S. Misc. Publ. No. 278 (1966).
76. W. L. Wiese, M. W. Smith, and B. M. Glennon, *Atomic Transition Probabilities, Vol. 1, Hydrogen Through Neon*, NSRDS-NBS 4 (1966).
77. V. P. Guinn, ed., *Proceedings of the International Conference on Modern Trends in Activation Analysis, College Station, Texas, April 19–22, 1965* (Texas A & MU., College Station, Texas, 1965); *Proceedings of the First Conference on Practical Aspects of Activation Analysis with Charged Particles, Grenoble, France, June 23, 1965* (Euratom, EUR 2957 d-f-e); R. S. Tilbury, *Activation Analysis with Charged Particles*, Nat. Acad. Sci.-Nat. Res Council, Nucl. Sci. Series, NAS-NS 3110 (Clearinghouse for Federal Sci. and Tech. Info., Springfield, Va., 1966); A. A. Smales, 'Radioactivity Techniques in Trace Characterization,' p. 307, in *Trace Characterization, Chemical and Physical*, W. W. Meinke and B. F. Scribner, eds., Nat. Bur. Stand. Monograph 100 (U.S. Govt. Printing Office, Washington, D.C., 1967); V. P. Guinn, 'Nuclear Methods,' p. 337, in *Trace Characterization, Chemical and Physical*, W. W. Meinke and B. F. Scribner, eds., Nat. Bur. Stand. Monograph 100 (U.S. Govt. Printing Office, Washington, D.C., 1967); H. G. Ebert, ed., *Proceedings of the 2nd Conference on Practical Aspects of Activation Analysis with Charged Particles, Liège, Belgium, September 21–22, 1967* (Euratom, EUR 3896 d-f-e).
78. J. E. Strain, 'Non-Reactor Neutron Sources,' p. 33 in *Guide to Activation Analysis*, W. S. Lyon, Jr., ed. (D. Van Nostrand Co., Inc., New York, 1964).
79. M. Cuypers and J. Cuypers, *Gamma-Ray Spectra and Sensitivities for 14-MeV Neutron Activation Analysis* (Texas A & MU., College Station, Texas, April 12, 1966).
80. S. S. Markowitz and J. D. Mahony, *Anal. Chem.*, **34,** 329 (1962).
81. E. Shuster and K. Wohlleben, 'Nondestructive Determination of Carbon in Silicon through the $C^{12}(d, n)N^{13}$ Reaction,' p. 45, in *Proceedings of the 2nd Conference on Practical Aspects of Activation Analysis with Charged Particles, Liège, Belgium, September 21–22, 1967*, H. G. Ebert, ed. (Euratom, EUR 3896 d-f-e).
82. E. A. Wolicki and A. R. Knudson, *Int. J. Appl. Rad. Isotopes*, **18,** 429 (1967).
83. I. L. Morgan, p. 149, in *Proceedings of the First Conference on Practical Aspects of Activation Analysis*

with Charged Particles, Grenoble, France, June 23, 1965 (Euratom, EUR 2957 d-f-e).
84. J. Lindhard and M. Scharff, *Phys. Rev.*, **124,** 128 (1961).
85. J. Lindhard, M. Scharff, and H. Schiott, *Kgl. Dan. Vidensk. Selsk. Mat. Fys. Medd.*, **33,** No. 14 (1963).
86. J. Lindhard, V. Nielsen, M. Scharff, and P. V. Thompson, *Kgl. Dan. Vidensk. Selsk. Mat. Fys. Medd.*, **33,** No. 10 (1963).
87. J. A. Davies, J. Denhartog, L. Eriksson, and J. W. Mayer, *Can. J. Phys.*, **45,** 4053 (1967).
88. L. Eriksson, J. A. Davies, N. Johansson, and J. W. Mayer, *J. Appl. Phys.*, **40,** 842 (1969).
89. F. W. Martin, *Nucl. Instr. Methods*, **72,** 223 (1969).
90. e.g. J. C. Walker and Y. K. Lee, p. 131 in *Nuclear Research with Low Energy Accelerators* (Academic Press, New York, 1967).
91. H. Frauenfelder and R. M. Steffen, p. 997 in *Angular Correlation in Alpha-, Beta- and Gamma-Ray Spectroscopy II*, K. Siegbahn, ed. (North-Holland Publishing Co., Amsterdam, 1965).
92. A. E. Litherland and A. J. Ferguson, *Can. J. Phys.*, **39,** 788 (1961).
93. A. Z. Schwarzschild and E. K. Warburton, *Ann. Rev. Nucl. Sci.*, **18,** 265 (1968).
94. A. R. Poletti and D. B. Fossan, *Phys. Rev.*, **160,** 883 (1967).
95. e.g. L. Grodzins, R. R. Borchers, and G. B. Hagemann, *Phys. Letters*, **21,** 214 (1966); F. Boehm, G. B. Hagemann, and A. Winther, *Phys. Letters*, **21,** 217 (1966).
96. J. Braunsfurth, J. Morganstern, H. Schmidt, and H. J. Korner, *Z. Phys.*, **202,** 321 (1967).
97. R. G. Stokstad, R. A. Moline, C. A. Barnes, F. Boehm' and A. Winther, p. 699 in *Proceedings of International Conference on Hyperfine Interactions Detected by Nuclear Radiations* (North-Holland Publishing Co., Amsterdam, 1968).
98. H. R. Lewis, Jr., Thesis, University of Illinois, 1958.
99. J. R. Alonso, Thesis, MIT, 1967.
100. G. Goldring, p. 640 in Ref. 97.
101. O. Klepper, L. Lehmann, and H. Spehl, p. 767 in Ref. 97.
102. J. Lindhard, *Kgl. Dan. Vidensk. Selsk. Mat. Fys. Medd.*, **34,** No. 14 (1965).
103. J. U. Andersen, J. A. Davies, K. O. Nielsen, and S. L. Andersen, *Nucl. Instr. Methods*, **38,** 210 (1965).
104. Oak Ridge National Laboratory Photograph No. 86604.
105. H. E. Wegner (private communication).
106. J. M. Khan, D. L. Potter, and R. D. Worley, *Phys. Rev.*, **163,** 81 (1967).
107. E. Bøgh and E. Uggerhøj, *Nucl. Instr. Methods*, **38,** 216 (1956); J. A. Davies, J. Denhartog, and J. L. Whitton, *Phys. Rev.*, **165,** 345 (1968).
108. W. M. Gibson, F. W. Martin, R. Stensgaard, F. Palmgren Jensen, N. I. Meyer, G. Galster, A. Johansen, and J. S. Olsen, *Can. J. Phys.*, **46,** 675 (1968).
109. W. M. Gibson, J. U. Andersen, and E. Uggerhøj, paper presented at Conference on Radiation Effects in Semiconductor Components, Toulouse, France, March 1967.

Received 5 August 1970